BBA - General Subjects 1862 (2018) 2660–2673

Contents lists available at ScienceDirect

BBA - General Subjects

journal homepage: www.elsevier.com/locate/bbagen

Lysine as a heme iron ligand: A property common to three truncated hemoglobins from *Chlamydomonas reinhardtii*

Eric A. Johnson[a,1], Miranda M. Russo[a,1], Dillon B. Nye[a], Jamie L. Schlessman[b], Juliette T.J. Lecomte[a,*]

[a] T. C. Jenkins Department of Biophysics, Johns Hopkins University, Baltimore, MD 21218, United States
[b] Chemistry Department, U.S. Naval Academy, Annapolis, MD 21402, United States

ARTICLE INFO

Keywords:
2-over-2 hemoglobin
Heme reduction potential
Nitric oxide dioxygenase
Nuclear magnetic resonance

ABSTRACT

Background: The nuclear genome of *Chlamydomonas reinhardtii* encodes a dozen hemoglobins of the truncated lineage. Four of these, named THB1–4, contain a single ~130-residue globin unit. THB1, which is cytoplasmic and capable of nitric oxide dioxygenation activity, uses a histidine and a lysine as axial ligands to the heme iron. In the present report, we compared THB2, THB3, and THB4 to THB1 to gain structural and functional insights into algal globins.

Methods: We inspected properties of the globin domains prepared by recombinant means through site-directed mutagenesis, electronic absorption, CD, and NMR spectroscopies, and X-ray crystallography.

Results: Recombinant THB3, which lacks the proximal histidine but has a distal histidine, binds heme weakly. NMR data demonstrate that the recombinant domains of THB2 and THB4 coordinate the ferrous heme iron with the proximal histidine and a lysine from the distal helix. An X-ray structure of ferric THB4 confirms lysine coordination. THB1, THB2, and THB4 have reduction potentials between −65 and −100 mV, are capable of nitric oxide dioxygenation, are reduced at different rates by the diaphorase domain of *C. reinhardtii* nitrate reductase, and show different response to peroxide treatment.

Conclusions: Three single-domain *C. reinhardtii* hemoglobins use lysine as a distal heme ligand in both Fe(III) and Fe(II) oxidation states. This common feature is likely related to enzymatic activity in the management of reactive oxygen species.

General significance: Primary structure analysis of hemoglobins has limited power in the prediction of heme ligation. Experimental determination reveals variations in this essential property across the superfamily.

1. Introduction

The nuclear genome of the green alga *Chlamydomonas reinhardtii* harbors a dozen genes (named *THB1–12*) belonging to the truncated lineage of the hemoglobin superfamily. Each of these genes exhibits a different expression pattern [1,2], but the functions of the corresponding products and the advantages conveyed to the organism by the availability of multiple hemoglobins remain enigmatic. In prior work, we showed that *THB1* expression is under the control of NIT2 [3], a transcription factor that regulates nitrogen assimilation. In a link to

Abbreviations: 1D, one-dimensional; CtrHb, heme domain of *Chlamydomonas eugametos* LI637 hemoglobin; DEAE, diethylaminoethyl; DQF-COSY, double-quantum filtered correlation spectroscopy; DT, sodium dithionite; FAD, flavin adenine dinucleotide; Fd, spinach ferredoxin; FNR, ferredoxin-NADP$^+$ reductase; G6P, glucose-6-phosphate; GODCAT, glucose oxidase/catalase dioxygen scavenging system; GlbN, *Synechocystis* sp. PCC 6803 or *Synechococcus* sp. PCC 7002 hemoglobin; Hb, hemoglobin; HPD, Heme Protein Database; HSQC, heteronuclear single quantum coherence; I3S, potassium 5,5′,7-indigotrisulfonate; IPTG, isopropyl β-D-1-thio-galactopyranoside; LB, Luria-Bertani; MAHMA-NONOate, 6-(2-hydroxy-1-methyl-2-nitrosohydrazino)-*N*-methyl-1-hexanamine; NADPH, nicotinamide adenine dinucleotide phosphate; NCS, non-crystallographic symmetry; NIT1, *C. reinhardtii* nitrate reductase; NO, nitric oxide; NOD, nitric oxide dioxygenase; NOE, nuclear Overhauser effect; NOESY, nuclear Overhauser spectroscopy; PDB, Protein Data Bank; PEG, polyethylene glycol; pH*, pH uncorrected for isotope effects; rmsd, root-mean-square deviation; SAD, single-wavelength anomalous diffraction; SDS-PAGE, sodium dodecyl sulfate polyacrylamide gel electrophoresis; TAP, Tris-acetate-phosphate; TOCSY, total correlation spectroscopy; TE, Tris-EDTA; THB, truncated hemoglobin from *Chlamydomonas reinhardtii*; TLS, translation/libration/screw; TRACT, TROSY for rotational correlation times; TrHb1, Group 1 truncated hemoglobin; WT, wild-type

* Corresponding author.
E-mail address: lecomte_jtj@jhu.edu (J.T.J. Lecomte).
[1] These authors contributed equally to this work.

https://doi.org/10.1016/j.bbagen.2018.08.009
Received 1 June 2018; Received in revised form 6 August 2018; Accepted 8 August 2018
Available online 10 August 2018

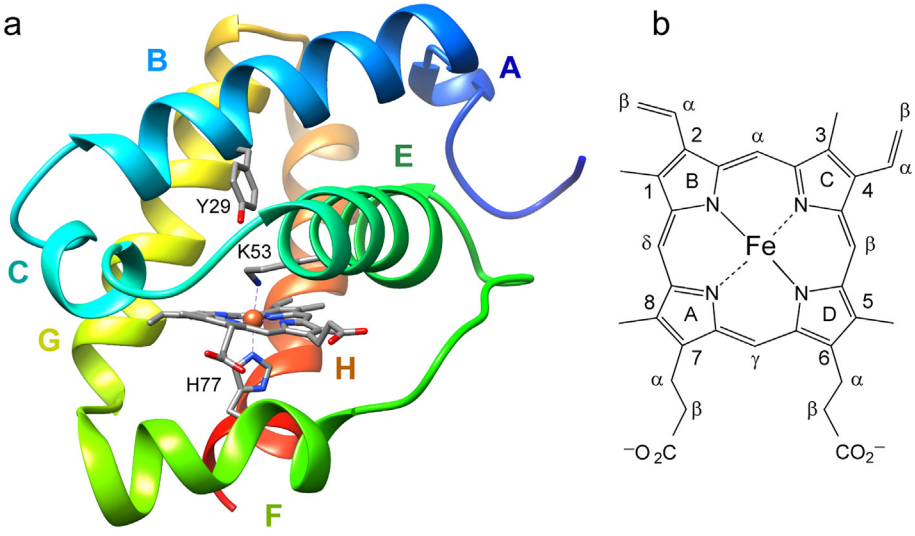

Fig. 1. (a) The X-ray structure of ferric THB1 (PDB ID: 4XDI, [5]) showing the proximal histidine (H77 or F8 in Perutz helical notation), distal lysine (K53 or E10), and tyrosine 29 (B10). THB1 has the typical truncated or 2-over-2 hemoglobin fold [8]. Helices are labeled A to C and E to H. (b) The heme group and nomenclature used in the text. The porphyrin ring supplies four pyrrole nitrogen ligands to the iron. Within a protein, the heme group can be found with no axial ligand (four-coordinate), one axial ligand (five- or pentacoordinate), or two axial ligands (six- or hexacoordinate). Typical iron oxidation states for a hemoglobin are Fe(II) (ferrous) and Fe (III) (ferric).

nitrogen metabolism, preliminary reactivity assays demonstrate that recombinant THB1 is capable of converting nitric oxide (NO) to nitrate (NO_3^-) in vitro under aerobic conditions [3]. This nitric oxide dioxygenase (NOD) activity is thought to occur in vivo [3,4]. Further in vitro characterization confirmed that THB1 has the fold of a Group I truncated hemoglobin (TrHb1) (Fig. 1a) and revealed a novel His–Fe–Lys coordination of the heme iron in both the Fe(III) (ferric) and Fe(II) (ferrous) states [3,5]. In the His–Fe–Lys ligation scheme, His is the conserved "proximal" histidine and Lys is the "distal" lysine (or Lys E10, Fig. 1a). Comparative information on additional THBs, including the identity of the heme axial ligands, is necessary to rationalize the multiplicity of globins in the alga.

We have proposed that distal lysine coordination is related to the ability of THB1 to detoxify NO efficiently. The chemical reason for this hypothesis is that the NOD reaction, which causes the oxidation of the heme iron from Fe(II) to Fe(III), requires THB1 to be reduced back to the active Fe(II) state [6]. The reduction step, a single electron transfer from a reductase, is energetically facilitated by a common set of iron ligands in the Fe(II) and Fe(III) oxidation states [7], and indeed electron self-exchange occurs rapidly in mixtures of Fe(II) and Fe(III) THB1 [3]. On the other hand, the relatively high pK_a of lysine, which must be deprotonated to coordinate the iron, results in a mixture of His–Fe and His–Fe–Lys complexes at neutral pH, with the pentacoordinate His–Fe form primed for exogenous ligand binding.

If Lys E10 assists in reactions that demand both redox chemistry and substrate binding, His–Fe–Lys coordination is not the only scheme up to the task. This is illustrated by variants of THB1 lacking this residue [3] and relatives of THB1 having His–Fe ligation or His–Fe–His ligation, which are all capable of some NOD activity [9,10]. Furthermore, a histidine at position E10 can also serve as a ligand in both iron oxidation states, presumably at a lower energetic cost than a lysine because the pK_a of histidine is close to physiological pH. Other endogenous ligation schemes have been proposed in TrHbs, including an elusive His–Fe–Tyr arrangement [11]. Thus, the characteristics and limitations of these various distal configurations merit further scrutiny.

In the present work, we extend our investigation of *C. reinhardtii* hemoglobins to the remaining single domain TrHb1s: THB2, THB3, and THB4. THB2 is predicted to be cytoplasmic and appears to be under the control of the same nitrogen metabolism transcription factor as THB1 [4]. However, whereas NO donors enhance the levels of THB1, they depress those of THB2. Recent transcription studies in *C. reinhardtii* have also linked up-regulation of both THB1 and THB2 to deprivation of nutrient sulfur [12]. While the two globins demonstrate distinct expression patterns, both are implicated in NO-linked regulation within the cell. THB3 belongs to a small subgroup of globins [13] that align strongly to known globin sequences, yet lack the hallmark proximal histidine. To our knowledge, the structural and chemical characteristics imparted by the absence of proximal histidine to this subgroup of globins have not been examined. THB4, the last protein considered in the present study, has been only partially characterized [14]. As with THB1, functional hypotheses advanced for THB4 center on nitrogen metabolism.

```
                                                    AAA  BBBBBBBBBBBBBBBBB     CCCC     EEEEEEEEEEEEEEEE
THB1      1-62   -------------------MAA---DTAPADS-LYSRMGGEAAVEKAVDVFYERIVADPQLAPFFANVDMKKQRRKQVAFMTYVF
THB2      1-79   -----MSPAPETVVAEPVAAAAGVVDAAAPPS-IFDRLGGEAAVEKAVDVFYERIVADPQLAPFFEGVDMRTQRRKQQAFMTYAF
THB3  116-200    APLNPAKLKLLKAATGLPVHTTSIGRRASASYCVYESMGGWETLSAAVESLYNRMRGDGRCASLFSEGNEQQLKTHMLEFLTCAL
THB4      1-85   MQSTPQANAAPANVNGSVSSAGQSKSAATTRSTLHAKLGGAAAVAATVDVFYKKLMNDPDLEPFFRGVDMVTLIAKQNRFLAYAF
LI637    12-96   PCIRAQQQPVRPSTSATAAAATAPAPARKCPSSLFAKLGGREAVEAAVDKFYNKIVADPTVSTYFSNTDMKVQRSKQFAFLAYAL

                                  FFFFFFFFFFFF   GGGGGGGGGGGGGGGGG    HHHHHHHHHHHHHHHHHHH
THB1    63-136   GGSGAYEGRDLGASHRRLIREQGMNHHHFDLVAAHLDSTLQELGVAQELKAEAMAIVASARPLIFGTGEAGAAN
THB2    80-147   GGATGYTGRDLAAAHRRLIRDKGLKEEHFDMVAGHLAGTLQLLGIGADLVDEVIALVATTKPVIFERV
THB3  201-268    GGKARFASSTLLTSQRDQLRQHGFGVGQFDILLQHMKAVLDEIGVQQETAASAIALLRCHKYLFERRQ
THB4    86-170   GATTHYHGKDIVMGHAHLIINRGLNLTHFDKVAGHFVDSLKEMGVGQELIDEAAGVLIGVRPLFDPERYKGKVDVEKIEKAATTP
LI637   97-164   GGASEWKGKDMRTAHKDLVPH--LSDVHFQAVARHLSDTLTELGVPPEDITDAMAVVASTRTEVLNMPQQ

THB4   171-188   QSKPAEAGQDAPACCTIM
```

Fig. 2. The primary structure of *C. reinhardtii* THB1–THB4 and *C. eugametos* LI637 (CtrHb). In Perutz notation, key positions (bold) are tyrosine "B10" (Y29, Y46, Y167, Y52, and Y63, respectively), the "E10" residue (distal, K53, K70, H191, K76, and K87, respectively), and the "F8" residue (proximal, H77, H94, Q215, H100, and H111, respectively). Four cysteines are underlined in THB3. Italics are used for the portions of sequence that were not included in the expressed recombinant proteins. The letters above the top sequence refer to the helices present in the X-ray structure of THB1 (Fig. 1a).

Fig. 2 displays the amino acid sequences of THB1–THB4. Compared to THB1 and using BLAST [15], THB2 has 66% identity (over 118 residues), THB3 has 29% identity (over 110 residues), and THB4 has 45% identity (over 116 residues). Both THB2 and THB4 have a lysine at position E10, which is a potential ligand to the iron on the distal side. As in His–Fe–His globins [16], however, the degree of distal coordination is expected to vary among proteins, with modulated consequences for exogenous ligand binding, dioxygen processing, and electron transfer reactions. In contrast, THB3 has a distal histidine that could coordinate the iron and compensate for the absence of a proximal histidine, but no probable lysine ligand. In this work, our practical goal was to determine the mode of iron ligation in the three single-domain THBs and compare them to each other and to the previously characterized THB1. In addition, to serve as a basis for the relationship between structure and function in this set of algal proteins, we establish basic physico-chemical properties known to condition heme reactivity.

2. Materials and methods

2.1. Protein preparation

2.1.1. THB1, THB2, and THB4

THB1 was prepared as previously reported without protocol modification [3]. The predicted protein sequences of THB2 (Cre14.g615350) and THB4 (Cre04.g218750) were aligned with known TrHb1 sequences to identify the conserved globin domains within the proteins (Fig. 2). Genes for these domains (entire THB2 1–147 and THB4 32–159) were then codon-optimized for expression in *E. coli*, synthesized, and inserted within the pJ414 plasmid (ATUM, Newark, California, USA) to generate the pTHB2 and pTHB4 plasmids. Several variants were obtained through mutagenesis of the pTHBn plasmids, using primers (Integrated DNA Technologies) listed in Supplementary Information Table S1 and either Q5 polymerase (New England BioLabs) or QuikChange mutagenesis (Agilent).

Wild-type (WT) THB2 and variants were prepared recombinantly from plasmid-containing *E. coli* strain BL21(DE3), grown at 37 °C with constant vigorous shaking in LB or M9 medium. Growth media were supplemented with 100 μg/mL ampicillin, and protein expression was induced with 0.5 mM IPTG for either 8–10 h (LB) or 10–12 h (M9). Following sedimentation by centrifugation, cell pellets were lysed in 50 mM Tris-HCl pH 7.5, 1 mM EDTA (TE buffer) with a probe sonicator (Qsonic). The insoluble inclusion bodies (containing the recombinant protein) were isolated by centrifugation and washed first in TE buffer with 0.5% Triton-X, then with TE buffer. The protein was suspended in TE buffer with 8 M urea and stirred gently for 45–60 min. 500 units of Benzonase® nuclease (MilliporeSigma) was added to the urea suspension to digest contaminating DNA. The protein solution was passed over a 100 × 2.5 cm G-50 Sephadex column equilibrated with TE buffer to remove the urea and refold the protein. The solubilized, refolded apoprotein was concentrated by pressure filtration (Amicon) using a 3 kDa molecular weight cutoff membrane and converted to holoprotein by addition of excess porcine hemin chloride (Sigma) dissolved in 0.1 M NaOH. The holoprotein was further purified, and excess heme removed, through binding to a 10 × 2.5 cm DEAE Sephacel anion exchange column equilibrated with TE buffer followed by elution using an NaCl gradient. Fractions were pooled and concentrated for exchange into 5 mM sodium phosphate pH 7.1. The resulting protein was checked for purity by SDS-PAGE and lyophilized for storage at −20 °C.

Mass spectrometry analysis of recombinant THB2 (Acquity/Xevo-G2, Waters) revealed that the material obtained from inclusion bodies of recombinant WT protein partitioned among three species, each with a different initial amino acid (Met, Ser, or Pro, Fig. 2). This is attributed to the presence of a proline at position 3 (P2'), which decreases the efficiency of *E. coli* methionine aminopeptidase MetAP1 [17]. Accordingly, the P3A (MSPA → MSAA) substitution variant and the S2_P3insA (MSPA → MSAPA) insertion variant of THB2 were generated. These proteins were obtained in monodisperse form and confirmed the origin of the multiple masses in the recombinant WT preparation. At this time, it is not known if the terminal methionine is cleaved in the *C. reinhardtii* cell, and whether the terminal residue is acetylated as observed for THB1 [18]. We were unable to attribute specific consequences to N-terminus heterogeneity and used the WT, P3A and S2_P3insA proteins interchangeably.

Slight variations in the appearance of the Fe(III) electronic absorption spectrum were observed at neutral pH with different inclusion body preparations of THB2. These variations, which disappear at high pH or upon reduction to the Fe(II) state, have an unknown origin. Imperfect reproducibility of cofactor binding is occasionally observed in the preparation of heme proteins [19] including monomeric hemoglobins [20]. As a control, a small amount of holoTHB2 produced by *E. coli* BL21 cells was purified. The optical properties of this holoprotein were consistent with those presented here for material prepared from inclusion bodies.

Recombinant THB4 globin domain and variants were obtained using a similar protocol with minor modifications to improve solubility. Protein expression was induced for 7 h in M9 medium; TE buffer at pH 8.0 was used throughout the lysis and purification; and the purified protein was exchanged into 5 mM sodium phosphate pH 7.5 before lyophilization. The anion exchange column was omitted for K76A THB4 because weak heme binding resulted in heme loss across the column. Uniformly ^{15}N-labeled proteins were prepared with $^{15}NH_4Cl$ as the sole nitrogen source in M9 medium. The extinction coefficient of THB2 and THB4 was determined with the Fe(III) protein on a per-heme basis at pH 7.5 using the hemochromogen assay [21]. Extinction coefficients at different pH or in the Fe(II) state were obtained from this reference state using titration curves corrected for dilution.

2.1.2. THB3

The *THB3* gene (Cre04.g218800) is linked to two different amino acid sequences in the Uniprot database, A8ISQ0 (218 aa) and R9S068 (297 aa). We designed the recombinant protein to encompass the common hemoglobin domain (144–268, following the numbering of the R9S068 sequence). The primary structure was further modified by replacing four Cys with Ser, at positions 147, 176, 196, and 259 (underlined in Fig. 2). We refer to this modified globin domain as THB3-S4. To aid in purification, the N-terminus included a His_6 tag, a FLAG antibody tag, and a PreScission Protease cut site. The resulting amino acid sequence was converted to a DNA sequence codon-optimized for expression in *E. coli*, and the DNA sequence was custom-synthesized for insertion within the pJ414 plasmid (ATUM).

Recombinant apoTHB3-S4 was expressed over a 9-h course following induction with 0.5 mM IPTG. The highly soluble apoprotein was bound to nickel-NTA agarose, released from the agarose column with 100 mM imidazole, and dialyzed overnight against 50 mM Tris-HCl buffer pH 8.0. During dialysis, PreScission protease, also tagged with His_6, was added to the apoTHB3-S4 solution to a final concentration of approximately 0.1 mg/mL. Following overnight digestion, both the cleaved apoprotein's histidine tag and the His_6-tagged protease were bound with nickel-NTA agarose, and the untagged apoprotein was eluted with 50 mM Tris-HCl pH 8.0. The purified THB3 apoprotein was pooled, concentrated, and analyzed by SDS-PAGE and mass spectrometry as with the THB2 and THB4 holoproteins. Elimination of free imidazole, which can have complicating effects in downstream applications (e.g., by binding to heme), was confirmed to sub-mM concentration by NMR spectroscopy.

2.1.3. Nitrate reductase extracts from C. reinhardtii

Partially purified nitrate reductase (NIT1) was obtained from cultures of *C. reinhardtii* according to published protocols [22]. 3.5 L of *C. reinhardtii* strain CC1690 was grown in TAP2/5 medium (Tris-acetate-phosphate medium with a modified nitrogen source of 2 mM NH_4^+ and 5 mM NO_3^-) under 12 h/12 h light/dark cycle until cell density

reached roughly 4 × 10^6 cells/mL. Following sedimentation by centrifugation, the cell pellet was flash-frozen in liquid nitrogen, thawed, resuspended in 20 mL of 20 mM Tris pH 7.5, 20 mM NaCl, then flash frozen in liquid N_2 again. The suspension was thawed on ice and then centrifuged at 4 °C for 15 min at each of the following accelerations: 7000 × *g*, 12,000 × *g*, 15,000 × *g* and 17,000 × *g*. After each centrifugation step, the supernatant was transferred to a fresh tube so as not to disturb the pellet. The resulting purified extract was then passed over a DEAE Sephacel column (GE) and eluted using a 20–500 mM NaCl gradient. Fractions containing nitrate reductase activity were identified with the Griess assay [23]. Positive fractions were pooled, exchanged into 20 mM Tris buffer pH 7.5, 20 mM NaCl, and concentrated to 1 mL. 100 µL aliquots were flash frozen in liquid nitrogen and stored at −80 °C until use.

2.2. Circular dichroism spectra

Circular dichroism spectra of apoTHB3-S4 (~12 µM, 25 mM sodium phosphate pH 7.0) and THB4 (15 µM, 10 mM sodium phosphate pH 7.6) were collected using an Aviv Model 420 spectropolarimeter. Spectra were collected over the range of 300 to 190 nm in 1 nm steps using a 3-s averaging time. The sample temperature was maintained at 25 °C. Thermal denaturation of THB3-S4 (~2 µM, 25 mM sodium phosphate, pH 7.0) was monitored by the change in ellipticity at 222 nm as the temperature was raised from 10 °C to 98 °C in steps of 1 °C allowing 1 min of equilibration between temperature increments.

2.3. pH titration monitored by electronic absorption spectroscopy

Titrations of THB2 and THB4 were performed as previously reported [3] with a Cary50 UV–Vis spectrophotometer (Agilent Technologies). Titrations in the Fe(II) state were conducted by addition of 2 mM sodium dithionite (DT, Alfa-Aesar) to separate ~15 µM Fe(III) samples prepared in 100 mM 2-(*N*-morpholino)ethanesulfonic acid buffer (pH 5–6.75), Tris buffer (pH 7–8.75), or glycine buffer (pH 9–10). Optical spectra were first collected in the Fe(III) state, and then in 30 s intervals over 10–15 min following DT addition. Data points for the pH titration curve were selected from each time course when the Soret absorbance was maximized, suggesting complete reduction. Both THB2 and THB4 displayed time-dependent spectral changes consistent with DT-induced damage, as observed with THB1 [3] and *C. eugametos* CtrHb [24].

2.4. Redox potential measurement

The reduction potential of each recombinant globin domain was determined using a modified version of published protocols [25,26]. Briefly, 1 mL of 100 mM sodium phosphate pH 7.0 in a quartz cuvette with Teflon stopper was deoxygenated with the glucose oxidase/D-(+)-glucose/catalase (GODCAT) system. Individual components included (final concentrations): 40 µg/mL bovine catalase (Sigma-Aldrich), 100 µg/mL *Aspergillus niger* glucose oxidase (Sigma-Aldrich), and 11 mM D-glucose. An oxygen electrode confirmed that at these concentrations, the GODCAT system depleted most dissolved O_2 in a small solution volume within < 5 min.

The deoxygenated solution was supplemented with 180 µM xanthine followed by 10 µM of the appropriate TrHb1 in the oxidized state. Aliquots of 1 mg/mL of potassium 5,5′,7-indigotrisulfonate (I3S) (MilliporeSigma) in water were added until the absorbance at λ_{max} = 596 nm was roughly equivalent to the absorbance of the Soret peak of the TrHb1. The spectrum of this solution was taken as the fully oxidized reference. 0.5 µL of xanthine oxidase (approximately 7 mU of an ammonium sulfate suspension, MilliporeSigma) was then added to the cuvette and spectra taken every min over 2 h as the solution was slowly reduced.

It is customary to add DT at the end of the experiment to obtain the spectrum of the fully reduced mixture [26]. However, the use of DT led to unreliable information, perhaps because of chemical damage. In addition, spectral overlap of the protein and the dye prevented the use of the two-wavelength absorbance equation generally applied to process the data. Instead, a basis set of four spectra (oxidized and reduced protein, and oxidized and reduced dye) was obtained at the appropriate concentration, and each spectrum collected during the reduction experiment was deconvoluted into a linear combination of these four species. The coefficients of the fit were then used to obtain the ratio of oxidized protein (dye) concentration to reduced protein (dye) concentration. The equilibrium Nernst equation,

$$E_{m,D} + \frac{RT}{n_D F} \ln\left(\frac{[D_{ox}]}{[D_{red}]}\right) = E_{m,P} + \frac{RT}{n_P F} \ln\left(\frac{[P_{ox}]}{[P_{red}]}\right) \quad (1)$$

where D refers to the dye and P to the protein, was assumed to hold over a sufficient portion of the reduction experiment. The number of electrons was set to $n_D = 2$ and $n_P = 1$ and the constant RT/F to 25.693 mV. Plots of (RT/2F) ln ($[D_{ox}]/[D_{red}]$) versus (RT/F) ln ($[P_{ox}]/[P_{red}]$) were generated, and $E_{m,P}$ extracted from the y-intercept of the straight line (equal to $E_{m,P} - E_{m,D}$) with the known redox potential at pH 7.0 of I3S (−81 mV, [27]). Only a portion of data points, describing a line corresponding to eq. 1, was used. We note that I3S was chosen despite suboptimal kinetic and spectral properties because its potential was close to that of the three proteins of interest. Along with the possibility of protein–dye association, these features render the reported reduction potentials approximate. E_m values are referenced to the standard hydrogen electrode.

2.5. Reduction assays

Two reduction systems were compared. The first was composed of the heme-free diaphorase domain of *C. reinhardtii* NIT1, which was prepared recombinantly as described previously [10]. The second was a crude cell extract of partially purified NIT1. For reduction using the NIT1-diaphorase domain, 50 nM of the recombinant protein was added to a Teflon-sealed cuvette containing 100 mM sodium phosphate buffer pH 7.5, the GODCAT system, and 150 µM NADPH. The solution was left to incubate at room temperature for several minutes to allow the consumption of dissolved oxygen and reduction of the NIT1-diaphorase domain. 10 µM of the appropriate TrHb1 was then introduced to the solution and the visible spectrum was scanned at 30-s intervals for 60 min. As a control experiment, each of the TrHb1s was incubated with the heme-less diaphorase domain (in equimolar concentration, 5 µM) for 5 min. In the reduced state, the electronic absorption spectrum of the heme-loaded cytochrome within the diaphorase is distinguishable from the spectra of the TrHb1s. Reduction with DT post-incubation showed no transfer of heme to the apocytochrome.

Experiments using native NIT1 were conducted in the same manner; however, because the NIT1 content of the crude extract was not precisely known, the amount of extract used in each experiment was determined by finding the volume of extract necessary to give roughly equivalent time of reduction for THB1 relative to the recombinant NIT1-diaphorase domain. This amount of extract (20 µL per 1 mL solution) was used to test each TrHb1. Each aliquot of extract was taken from the same stock to allow qualitative comparison.

2.6. Nitric oxide dioxygenase assay

THB1, 2, or 4 (10 µM, 100 mM sodium phosphate, pH 7.5) was incubated in O_2-saturated buffer (O_2, Airgas) with the following components (MilliporeSigma): 50 mU spinach ferredoxin $NADP^+$ reductase (FNR), 0.5 µM ferredoxin (Fd), 40 µg/mL catalase and 180 µM NADPH [28]. NADPH alone failed to reduce any of the TrHb1s used in these experiments. In the presence of the reductase system the proteins convert to their oxy (Fe(II)–O_2) form. Conversion was followed

optically and when completed, MAHMA-NONOate (Cayman Chemicals, Ann Arbor, MI) was added to 2-fold molar excess of NO (on a heme basis) to generate NO and initiate NOD activity. After oxidation, the TrHb1s undergo re-reduction by the enzyme system and return to the Fe(II)–O_2 form. For multiple NO addition experiments, MAHMA-NONOate was introduced after nearly full recovery to the Fe(II)–O_2 form. This protocol differs from that originally used for THB1 (Fd-FNR system with glucose-6-phosphate (G6P) and G6P dehydrogenase to regenerate NADPH from $NADP^+$ [3]) and is identical to that used in a *Synechococcus* GlbN study [10] except for a higher concentration of FNR.

2.7. Treatment with hydrogen peroxide

To compare the resistance of THB1, THB2, and THB4 to hydrogen peroxide, a stock solution of 10 mM H_2O_2 was made from a 30% solution (Sigma-Aldrich) with the final concentration determined using an extinction coefficient of 39.4 M^{-1} cm^{-1} at 240 nm [29]. The stock was then added to a 10 μM solution of protein buffered with 100 mM sodium phosphate (either pH 7.0 or pH 8.0 as noted) to a final concentration of 50 μM H_2O_2. The electronic absorption spectrum of the solution was followed every 30 s for 2 h.

2.8. NMR spectroscopy

NMR samples of Fe(II) THB2 or THB4 were prepared by reduction of 0.5–2.5 mM protein with 3–4 molar equivalents of DT (concentration determined optically using the extinction coefficient $\varepsilon = 8$ mM^{-1} cm^{-1} at 314 nm [30]) in a glove box as described previously [3]. Samples were in 20–50 mM sodium borate buffer (pH 10), or 20–50 mM sodium phosphate buffer (pH 7.2–7.5) in either 90% ^1H_2O/10% ^2H_2O or 90% ^2H_2O/10% ^1H_2O (pH* 7.2–7.5). WT and Y46F THB2 spectra were acquired with a Varian Inova 800 MHz spectrometer. P3A THB2, P3A K70A THB2, THB3, and THB4 spectra were collected on a Bruker Avance or Avance II 600 MHz spectrometer equipped with a cryoprobe. ^1H chemical shifts were referenced to 2,2-dimethylsilapentane-5-sulfonic acid through the ^1H_2O line (4.76 ppm at 298 K). ^{15}N chemical shifts were referenced indirectly using the Ξ ratios [31]. NMR data were processed using NMRPipe 3.0 [32] or TopSpin 3.5 (Bruker Biospin, Rheinstetten, Germany) and assignments were made using Sparky 3 [33].

^1H–^1H NOESY (mixing time 75 ms), ^1H–^1H DQF-COSY, ^1H–^1H TOCSY (mixing time 35–45 ms) data were acquired as previously described to assign the heme and heme pocket resonances (see for example our work on THB1 [3]). To examine the upfield resonances arising from the distal lysine, additional ^1H–^1H TOCSY data were collected with the ^1H carrier frequency at −2.5 ppm and with a shortened mixing time (27–30 ms). The ^1H–^{15}N HSQC spectrum of THB4 for lysine $^{15}N\zeta H_2$ detection was collected with an ^{15}N carrier frequency of −40 ppm and a ^1H carrier frequency of −8.75 ppm. Water suppression in the ^1H–^{15}N HSQC experiments was achieved with a selective 180° final pulse with a null at the water frequency.

1D-TRACT experiments [34] were performed on THB4 as previously described [35], at various THB4 concentrations (0.5–2 mM), pH (7.5 or 8), temperature (298 K or 310 K), and states (Fe(III), Fe(II), or Fe(III)-CN). For each condition, 8 to 12 time points for the relaxation period were collected for both the TROSY (α) and anti-TROSY (β) components. To assess the quality of the data, two time points were duplicated for each data set. The amide signals were integrated using Topspin 3.5. Correlation times were calculated using an in-house program [35].

2.9. X-ray crystallography

THB4 crystals were grown at room temperature using the hanging drop vapor diffusion method, with 0.5 mL of solution in the reservoir. 3 μL of 33 mg/mL THB4 in the ferric state was mixed with 1 μL of reservoir solution, consisting of 0.2 M ammonium sulfate, 0.1 M Bis-tris pH 5.5, and 20% PEG 3350. Red crystals, measuring ~0.35 × 0.35 × 0.2 mm^3, appeared within 12 h. Single crystals were looped and coated in Paratone oil prior to flash-cooling in a chilled nitrogen stream. Data were collected at 110 K on a Rigaku Oxford Diffraction Super Nova X-ray diffractometer using CuKα radiation. CrysAlisPro was used for data indexing, integration and scaling.

Phenix.autosol, phenix.refine, [36] and coot [37] were used for phasing, refinement, and model building, respectively. Initial phasing was solved by SAD using the anomalous signal of the heme iron. NCS restraints were used for the two polypeptide chains in the asymmetric unit during the initial rounds of refinement and released after three rounds of refinement. TLS was incorporated into the final two rounds of refinement, using two TLS groups (the A chain and the B chain). Crystal contact interfaces were analyzed using the standalone PISA software from the CCP4 suite [38]. MOLEonline v.2.5 was used for cavity calculation [39].

3. Results and discussion

3.1. Heme ligand identification in THB2

The electronic absorption spectrum of WT THB2 in the Fe(III) state near neutral pH is shown in Fig. 3a. The features include a weak charge transfer band at 623 nm and are consistent with a mixture of a low-spin His–Fe–X complex (with X representing an unknown distal ligand) and a small amount of a high-spin complex, likely His–Fe–OH_2. Reduction to the Fe(II) state with DT at pH 7.5 results in a spectrum exhibiting sharp, resolved α and β bands (Fig. 3a). These Fe(III) and Fe(II) spectra, which are obtained in the absence of added exogenous ligand, support that X coordinates the iron in both oxidation states. Spectral parameters for THB2 are listed in Table 1.

The data reported for Fe(III) THB2 in Table 1 differ from those published by Ciaccio and colleagues [14], although addition of excess imidazole to our preparations of THB2 nearly eliminates the discrepancies (Fig. S1). The properties of Fe(III) THB2 in the absence of added exogenous ligand were pursued further by NMR spectroscopy. The 1D ^1H NMR spectrum at pH 7 (Fig. S2) has sharp hyperfine shifted lines consistent with a low-spin complex (His–Fe–X). Negligible signals indicative of a high-spin or mixed-spin species ($\delta > 25$ ppm) are detected despite the presence of a charge transfer band in the electronic absorption spectra. Raising the pH to 11 reduces the intensity of these highly shifted signals and also diminishes the charge transfer band. However, the pH titration of Fe(III) THB2 monitored by ^1H NMR spectroscopy revealed the coexistence of more than two states across the whole pH range. Perhaps related to the variability noted with Fe(III) THB2 is the observation that this protein, like THB1 and a small number of TrHbs [40,41], has some affinity for acetate (Fig. S3), which suggests a permissive binding site using Tyr B10 for ligand stabilization. In contrast to Fe(III) THB2, Fe(II) THB2 behaves consistently with a shallow pH transition and an apparent pK_a of ~7 leading to a four-coordinate-like spectrum [24] via a five-coordinate intermediate (Fig. S4). This pH response is similar to that of THB1 [3].

The spectral appearance and primary structure (Fig. 2) point to K70 as a candidate for distal coordination (X in His–Fe–X). The replacement of a residue thought to be an axial ligand followed by the comparison of spectral features is a standard approach to probe the coordination scheme of a heme protein. Replacement of K70 with an alanine in the background of P3A THB2 led to an Fe(III) spectrum typical of a His–Fe–OH_2 complex at neutral pH (Fig. S5). Reduction with DT at neutral or alkaline pH yielded an electronic absorption spectrum displaying a broad Soret band at 426 nm and unresolved α and β bands at 557 nm (Fig. S5) in agreement with a mixture of five-coordinate “deoxy” species [42] and four-coordinate species [24]. The 1D ^1H NMR spectra of Fe(II) WT THB2 and Fe(II) P3A/K70A THB2 collected at pH 10.4 (Fig. S6) confirm a change from diamagnetic (WT THB2, sharp lines distributed over a narrow chemical shift range) to paramagnetic (P3A/

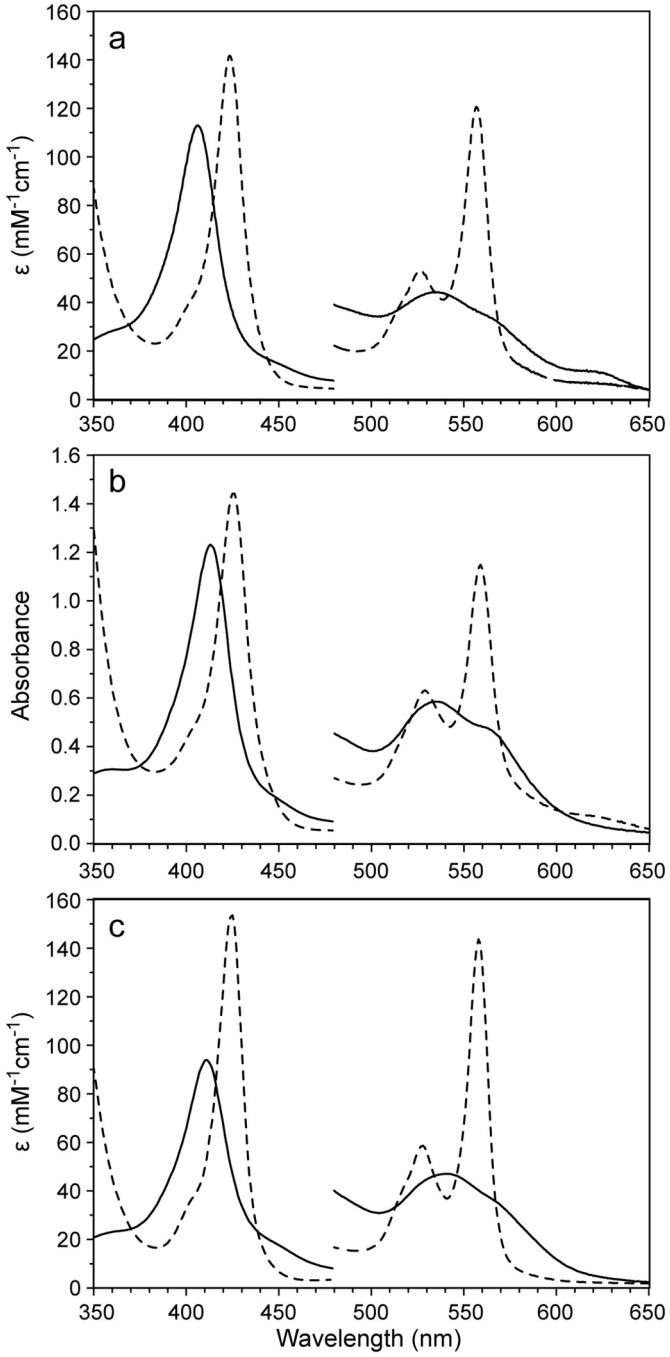

Fig. 3. Absorption spectra of 10–15 μM THB2 (a), THB3-S4 (b), and THB4 (c) in 100 mM (a, c) or 20 mM (b) Tris, pH 7.5. Fe(III) spectra are shown with solid lines and Fe(II) spectra are shown with dashed lines. The intensity of the region from 480 to 650 nm was magnified by a factor of 5. Extinction coefficients for THB2 and THB4 were obtained with the hemochromogen assay. Because of weak heme binding to THB3-S4 and unknown stoichiometry of the reconstituted material, the *y*-axis in b is absorbance.

K70A THB2, broad and highly dispersed signals).

Because targeted amino acid replacement, such as K70A THB2, can occasionally yield false positive or false negative results, direct information on the axial ligand was obtained with additional NMR characterization of WT Fe(II) THB2 at alkaline pH. Fig. 4a shows the 1D ^{1}H spectrum. The most upfield-shifted signals (−7.8 ppm) disappear when the protein is dissolved in 99% $^{2}H_2O$. These signals and several between −1.1 and −3.3 ppm form a set similar to that observed for Lys E10 (K53) in THB1 [3] and other proteins exhibiting lysine coordination [5,6,43,44]. The upfield shifted signals are also detected in Fe(II) THB2 at pH 7.0, but they are broadened, presumably because of exchange with the five-coordinate intermediate evidenced by electronic absorption spectroscopy. Homonuclear NOESY (Fig. 4b) and TOCSY (Fig. 4c) data in the upfield shifted region display *J*-correlations and dipolar contacts consistent with a lysine side chain, with the signal at −7.8 ppm arising from the amino group.

Table 1
Optical properties of WT THB2 and THB4 at pH 7.5.

Protein	State	Soret (ε)	β (ε)	α (ε)	CT
THB2	Fe(III)	406 (113)	535 (8.8)	560 (sh) (7.1)	622
	Fe(II)	424 (141)	526 (11)	557 (24)	
	Fe(II)-O_2	409	545	580	
THB4	Fe(III)	411 (94)	541 (9.4)	560 (sh) (7.8)	
	Fe(II)	425 (154)	528 (12)	558 (29)	
	Fe(II)-O_2	413	545	580	

Maximum wavelengths are in nm and extinction coefficients (ε) are in (mM^{-1} cm^{-1}); CT, charge transfer; sh, shoulder.

Heme resonances were assigned with the same data sets (Table S2). The spectra reveal that THB2 exists in a nearly 1:1 mixture of two species exchanging slowly on the chemical shift time scale. Dipolar contacts between heme and protein matrix are consistent with heme rotational isomerism, i.e., the coexistence of two forms related by a 180° rotation of the heme about the α–γ meso axis (Fig. 1b). Thus, THB2 shows no ability to discriminate between two possible modes of protein–cofactor interaction.

In THB1, replacement of the conserved tyrosine at the B10 position with a phenylalanine (Y29F variant) improves spectral quality [3]. The molecular origin of the improvement is unknown, but it is worth noting that in the structure of THB1 (PDB ID: 4XDI), the ring of Tyr B10 is at the interface of the B and E helices, and removal of the hydroxyl group is expected to disrupt a network of hydrogen bonds formed with water molecules and Gln E7. The corresponding replacement in THB2 (Y46F) was performed to gain additional resolution (Fig. S6, S7; Table S2). NOEs between the upfield shifted lysine and the heme (Fig. 4d) are clearly seen in the spectra of this variant protein and solidify the geometry of the side chain in each of the heme rotational isomers. We conclude that THB2 uses Lys E10 as a ligand in the Fe(III) and Fe(II) states, and that the endogenously coordinated species dominates at neutral pH.

3.2. Heme binding by THB3 variants

The globin domain of THB3 was prepared in pure, imidazole-free apoprotein form with four Cys replaced with Ser (hereafter THB3-S4) to improve the stability of the protein with respect to oxidation and facilitate its purification. Using the sequence alignments shown in Fig. 2, the locations of the four Cys are one in each of the pre-A region, BC turn, C-terminal end of the E helix, and the middle of the H helix. Based upon this alignment and structural models of known TrHb1 proteins, none of these residues appears positioned either to form disulfide bridges or to serve as a heme axial ligand within the canonical heme binding site. When hemin is added to apoTHB3-S4 in an approximately stoichiometric amount, a Soret peak at 412 nm emerges and stabilizes over the course of ~20 min. The appearance of the band at 412 nm is accompanied with the disappearance of the 380 nm signature of free heme. When this solution is exposed to DT, the Soret band sharpens and shifts to 426 nm, and resolved α and β bands emerge. These spectra are shown in Fig. 3b. Interestingly, Fe(III) THB3 does not show a detectable charge transfer band, which suggests that the heme has two strong-field protein ligands. However, when the reconstituted holoprotein was passed through a DEAE Sephacel column, only apoprotein was recovered. Subsequent attempts to titrate apoTHB3-S4 with heme indicated micromolar affinity (Fig. S8A). Replacement of the distal

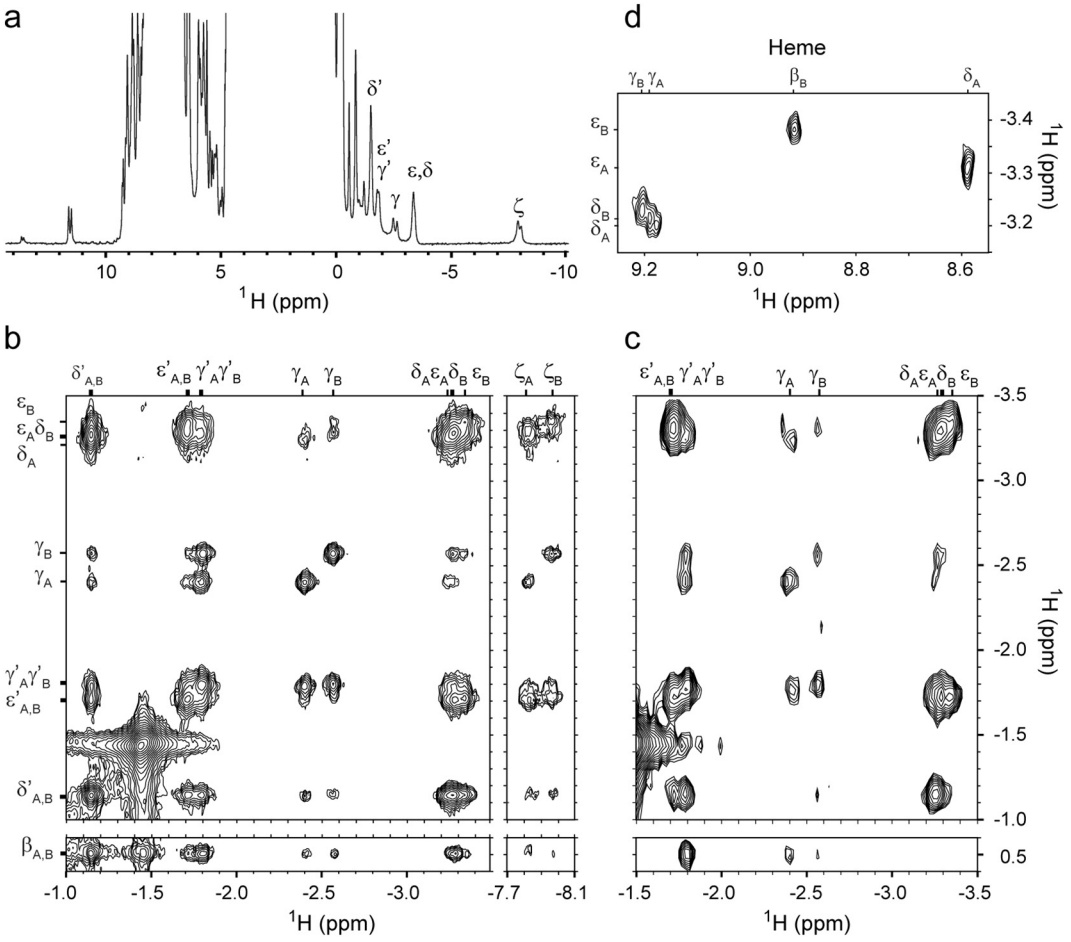

Fig. 4. NMR spectra of THB2 in the Fe(II) state at 25 °C. The heme orientational isomers are denoted A and B. (a) 1D ^{1}H spectrum of THB2 at pH 10.0 in 10% $^{2}H_2O$ / 90% $^{1}H_2O$ with resolved K70 resonances labeled. (b) Upfield region of ^{1}H–^{1}H NOESY data showing K70 resonances. (c) Portion of ^{1}H–^{1}H TOCSY data showing some of the connectivities of K70. (d) Portion of ^{1}H–^{1}H NOESY spectrum of Y46F THB2 at pH 10.0 in 100% $^{2}H_2O$ showing dipolar contacts between the heme meso protons (top labels) and K70. One of the K70 ε protons in the A form has contacts with the δ-meso proton of the heme, while the corresponding K70 ε proton in the B form contacts the β-meso proton of the heme, consistent with heme orientational isomerism. Assignment to specific protons of K70 is tentative, except for NζHs.

histidine with an alanine (H191A) weakened but did not abolish heme binding (Fig. S8B), whereas replacement of the proximal glutamine with a histidine (Q215H) in the THB3-S4 background intended to strengthen heme binding with bis-histidine coordination produced no marked change in the absorption spectrum. Restoration of the Cys residues at either the BC turn (position 176) or the E helix (position 198) yielded proteins with a tendency to aggregate and no obvious effect on heme association (not shown).

The data collected thus far do not identify heme ligands with certainty. It is possible that the heme is coordinated by H191 and Q215. However, coordination by a glutamine is rarely observed. In the A264Q variant of cytochrome P450 BM3, a structural model shows the proximity of the glutamine to the heme iron (PDB ID: 3EKF), with assumed amide oxygen coordination [45]. A recent study of HemQ from *Listeria monocytogenes* also proposes a glutamine ligation (glutamine 187 in the M149A variant), but apparently through the side chain amide nitrogen [46]. An alternative explanation for THB3 is that the heme does not bind in the expected site and recruits residues other than H191 and Q215 for axial ligation.

Although the electronic absorption spectra of the heme adduct of THB3-S4 were intriguing, weak heme association with the protein made further exploration challenging. Whether a physiological role of THB3 involves heme, as a cofactor or cargo, remains to be explored. It is noteworthy that circular dichroism data collected on apoTHB3-S4 show that the protein has a high helical content (Fig. S9). The NMR spectrum is well resolved at neutral pH and supports the presence of stable secondary and possibly tertiary structure (Fig. S9). Thermal denaturation of apoTHB3-S4 displays an apparent cooperative unfolding transition above 60 °C (Fig. S10), providing further support for a structured apoprotein. Thus, it is plausible that the protein is folded and capable of some function without a cofactor or perhaps in transient association with a heme group [47].

3.3. Heme ligand identification in THB4

Fig. 3c contains the Fe(III) electronic absorption spectrum of THB4, which at neutral pH has the appearance of a fully populated low-spin complex. Relative to THB1 and THB2, the spectrum of Fe(III) THB4 is remarkably unresponsive to pH, showing no change over the range of pH 6 to 11 (Fig. S11). The reduced state spectrum shows well-resolved α and β bands (Fig. 3c), also in support of a low-spin complex. In contrast to the relatively unresponsive pH behavior observed in the Fe(III) state, the pH response of THB4 in the Fe(II) state is nearly identical to that of THB1 and THB2, with a five-coordinate to four-coordinate conversion taking place at acidic pH (Fig. S12). The optical spectra of THB4 obtained here overlay well with published THB4 spectra in both the Fe(III) and Fe(II) states [14], with only minor differences around 670 nm that the authors attribute to impurities or heme *d*.

In THB4, the lysine homologous to the endogenous ligand in THB1 (K53) and THB2 (K70) is K76. The electronic absorption spectrum of Fe(III) K76A THB4 at neutral pH displays a weak charge transfer band and features somewhat resembling those of a His–Fe–OH_2 heme protein

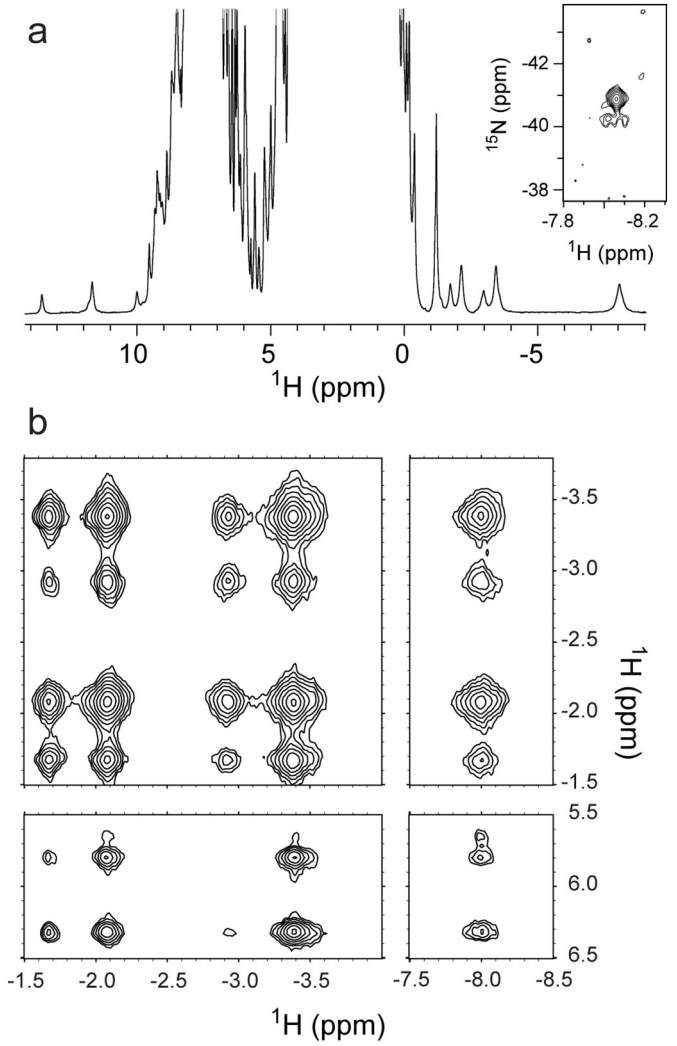

Fig. 5. NMR spectra of THB4 in the ferrous state in 10% $^{2}H_2O$ / 90% $^{1}H_2O$ at 25 °C. (a) 1D ^{1}H spectrum of THB4 at pH 10.0, showing the upfield resonances characteristic of lysine coordination, between −1.1 and −8.2 ppm. The NζH_2 of K76 is indicated at −8.1 ppm. Inset: Region of the ^{1}H–^{15}N HSQC spectrum at pH 7.5 showing the K76 NζH_2 resonances. (b) Upfield portion of the ^{1}H–^{1}H NOESY of THB4 at pH 10.0, showing some of the K76 dipolar contacts to itself and to Phe65.

(Fig. S13). At alkaline pH, the appearance of a band at 380 nm and the simultaneous loss of absorbance of the Soret band suggest a partially dissociated heme. Surprisingly, unlike the Lys E10 Ala variant of THB1 (K53A) or THB2 (K70A), passing the Lys E10 Ala variant of THB4 (K76A) through a DEAE Sephacyl column resulted in heme loss. Although these data demonstrate that K76 is important for heme binding and ligation, additional information was required to confirm it is indeed an axial ligand.

Sample NMR data collected on Fe(II) WT THB4 are shown in Fig. 5. The signature upfield signals of a His–Fe–Lys complex are readily recognized. Heme assignments (Table S3) as well as assignments of key residues in contact with the heme were obtained. In this protein, the heme orientational isomer ratio is 4:1. Unfortunately, rapid transverse relaxation limited the ability to collect and interpret THB4 NMR spectra. [^{15}N,^{1}H]-TRACT experiments, which provide an estimate of the effective rotational correlation time through cross-correlation effects [34], were performed to inspect the origin of the line broadening (not shown). A monomeric protein of the size and shape of the truncated globin domain should exhibit a TRACT correlation time of ~7 ns [48]. The data returned values ranging between 10 and 22 ns, which indicated some extent of association in solution at NMR concentrations. Interestingly, the cyanide-bound ferric state exhibited sharper lines and a correlation time of 8–9 ns, suggesting a difference in association state linked to the nature of the distal ligand and the conformational properties of the complexes.

Table 2
Data collection and refinement statistics for THB4 crystallography.

Data Collection	
Wavelength (Å)	1.54
Resolution range (Å)	20.68–1.90 (1.97–1.90)[a]
Space group	$P2_12_12$
Unit cell a, b, c (Å)	74.4, 68.3, 49.4
Unit cell α, β, γ (°)	90, 90, 90
No. of total reflections	325,393 (23841)
No. of unique reflections	38,306 (3832)
Multiplicity	8.5 (6.2)
Completeness (%)	99.9 (99.9)
Mean I/σ (I)	32.4 (5.0)
R_σ	0.028 (0.169)
Wilson B (Å^2)	17.8
Refinement	
Resolution range (Å)	20.68–1.90 (1.92–1.90)
Data cutoff (σ(F))	1.34
No. of unique reflections	38,227 (1307)
Completeness (%)	99.8 (97.0)
R_{free}	0.227 (0.225)
R_{work}	0.188 (0.303)
CC(work)	0.966 (0.917)
CC(free)	0.947 (0.907)
No. of atoms	2,233
Proteins	1,949
Ligands	96
Solvent	188
Protein residues	252
RMS bonds (Å)	0.008
RMS angles (°)	0.75
Ramachandran favored (%)	100
Rotamer outliers (%)	0
Clash score	4.18
B-factor (Å^2)	
Average	20.4
Proteins	20.3
Ligands	15.6
Solvent	24.6
Number of TLS groups	2

[a] Values in parentheses are for the high-resolution shell.

3.4. Structural model of THB4

3.4.1. General features

THB4, which has only 45% sequence identity with THB1 (Fig. 2), was chosen as a promising candidate to expand the diversity of available TrHb1 structures and provide a structural basis for distal lysine coordination. Fe(III) THB4 readily produces crystals in the $P2_12_12$ space group. The crystallographic asymmetric unit contains two protein molecules and the structure could be determined using single-wavelength anomalous diffraction from the heme iron for phasing. The final model was obtained to a resolution of 1.90 Å (PDB ID: 6BME) with the statistics for data collection and refinement included in Table 2.

The N- and C– termini are mostly unstructured, but the electron density is sufficient to model all of the residues in the A chain, except for the C-terminal residue (D159), and all but three N- and C-terminal residues in the B chain (S32, V158, and D159). Each protein molecule contains seven α-helical elements (A to C and E to H). The high helical content persists in solution as reflected in the shape and strength of the far UV circular dichroism spectrum (Fig. S14). The backbones of the two protein molecules align with an rmsd of 0.4 Å (125 Cα pairs). The largest deviations are located at the first 12 residues, the last 6 residues, and loops connecting helices. Fig. 6a shows a ribbon diagram of chain

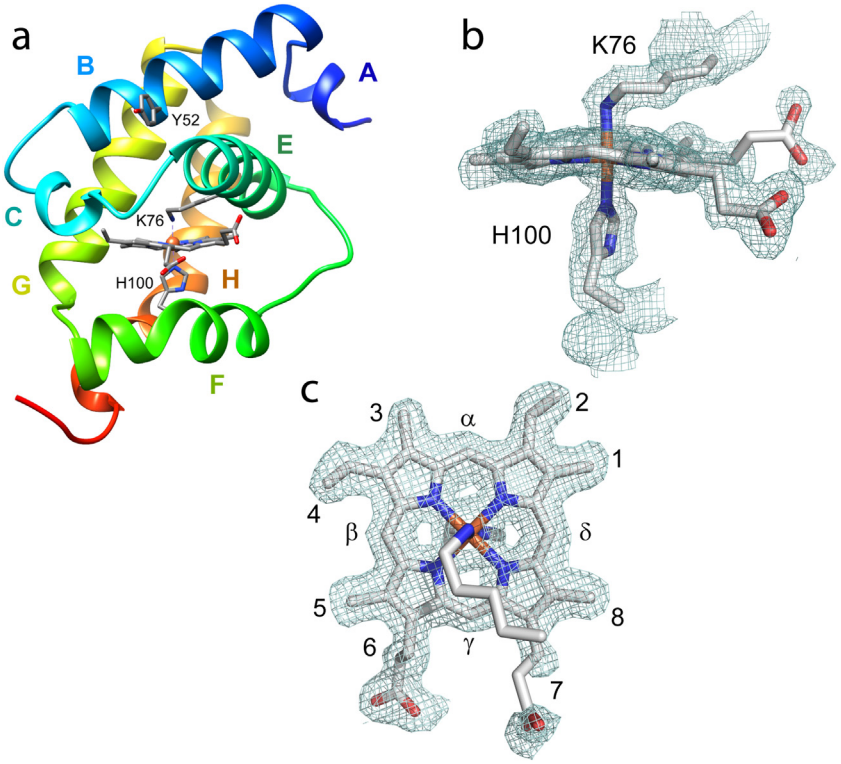

Fig. 6. (a) Ribbon diagram of THB4 (PDB ID; 6BME, chain A) with helices labeled. The axial heme ligands and Tyr B10 are indicated. (b,c): 2 $F_o - F_c$ electron-density map (contoured at the 1.0 σ level, chain A) of the heme and axial ligands. The electron density maps were prepared with PyMOL [49].

A.

3.4.2. The heme group and its axial ligands

The orientation of the heme group within the protein is well defined by the electron density (Fig. 6c). As concluded from the NMR data, one heme orientational isomer dominates, and this isomer is the same as the major species found in both THB1 (PDB ID: 4XDI, [5]) and *C. eugametos* TrHb-CN (PDB ID: 1DLY, [8]). As in most TrHb1s [50], the heme plane is slightly ruffled [51]. The heme propionates participate in hydrogen bonds with water molecules, but, unlike in THB1, there is no direct contact with protein residues. Ambiguity in the dihedral angles of the 7-propionate substituent could not be resolved with the current electron density map.

The coordination bond between the proximal histidine (His100) Nε2 atom and the iron is 2.0 Å in both chains. The imidazole plane is perpendicular to the average heme plane and such that the Cδ2–Cε1 direction is nearly aligned with the β-meso–δ-meso direction. This is a staggered orientation with respect to the nitrogen pyrroles, which minimizes steric strain [52] and is commonly found in TrHb1s. The electron density clearly designates K76 as the sixth ligand to the heme iron. The distance between the iron and the K76 Nζ atom is 2.1–2.2 Å. The dihedral angles of the side chains (χ1, χ2, χ3, and χ4) are approximately *trans*, *trans*, *trans*, and *gauche+*, which results in Fe–Nζ–Cε angles of 117°, consistent with the sp^3 hybridization of the Nζ atom and practically identical to the orientation of K53 in THB1.

3.4.3. Comparison to other TrHb1s

The globin domain of THB4 resembles other such domains, with a one-turn A helix, 3_{10} C helix (D58–D60), long EF loop, irregular F helix, and irregular C-terminal end to the H helix. Hallmarks such as the N-terminal caps of the C helix and E helix [53] and the backbone–histidine side chain hydrogen bond at the beginning of the G helix (N110–H113) [54] are all present, although there are some interesting variations as well. For example, the F helix of THB4 is similar to that of synechococcal GlbN (PDB ID: 4MAX, a protein with a distal histidine ligand [55]) but is extended by one turn on the N-terminal side compared to THB1. The kink in the H helix of THB4 also deviates from the THB1 structure and more closely resembles the C-terminus of GlbN.

Another distinctive feature of THB4 compared to THB1 is a rotation of the E helix about its long axis, which turns Tyr B10 (Y52) away from the heme cavity, as observed in GlbN. A comparison of the E helix illustrates a range of positions for these three proteins (Fig. 7). Tyr B10 is known to play a critical role in stabilizing bound exogenous ligand [56,57]. In the His–Fe–Lys state of THB1, this residue participates in a network of hydrogen bonds involving Gln E7 and water molecules. In THB4, position E7 is occupied by a leucine, which points to the inside of the heme cavity. We speculate that the absence of a residue capable of hydrogen bonding at position E7 has a role to play in determining the relative orientation of the B and E helices and the positioning of Tyr B10.

Many TrHb1s display tunnels thought to be used by small ligands to gain access to the active site [58]. Often, these tunnels are apparent only when the protein has an exogenous ligand bound [50,59] and when gating residues, such as Phe E15 in *M. tuberculosis* HbN [58,60,61], adopt the proper rotameric state. A search for tunnels in the structural model of THB4 reveals a short channel in chain A between the C-terminal end of the B helix and the N-terminal end of the E helix (Fig. S15). Interestingly, Tyr B10 borders the channel, and Phe CD1 (F65 at the end of the 3_{10} C helix) along with Leu E7 prevent the opening from reaching the heme group. It is likely that, as in other TrHb1 with endogenous distal ligand, this (or other channels) opens when an exogenous ligand is present. In the His–Fe–Lys state, however, THB4 appears less porous than THB1 (Fig. S15). Unlike with THB1 and THB2, exposure of THB4 to high concentration of acetate does not lead to an acetate-bound state (Fig. S3).

3.5. Redox potential measurements

The His–Fe–Lys coordination scheme is not frequently observed, and the physico-chemical properties of this type of complex are

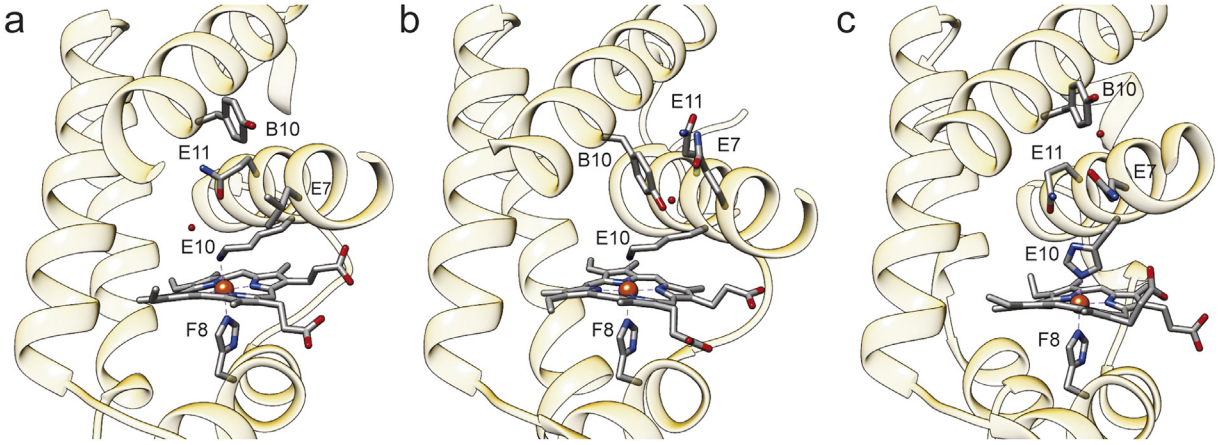

Fig. 7. Comparison of the heme binding pockets of (a) THB4 (PDB ID: 6BME), (b) THB1 (PDB ID: 4XDI), and (c) *Synechococcus* GlbN (PDB ID: 4MAX) showing the axial ligands (E10 and F8), key residues B10, E7, and E11, and water molecules near residue B10 or E10.

incompletely described. To begin the characterization of TrHb1s with His–Fe–Lys ligation and gain insight into their reactivity, we measured the reduction potentials of these proteins. Using the method developed by Massey [25], but with the GODCAT system to maintain microoxic conditions [62], we monitored the reduction of THB1, THB2 and THB4 relative to a known redox-sensitive dye. Following several attempts to find a dye with the proper redox poise, I3S (E_m = −81 mV, [27]) was selected. Typical data are shown in Fig. 8. The measurements yielded reduction potentials of −67 mV, −90 mV, −98 mV, for THB1, THB2, and THB4, respectively, with a 1 mV uncertainty derived from triplicate experiments.

In the potential range of the three THBs, the Heme Protein Database (HPD) [63] lists half a dozen examples of *b* heme proteins (His–Fe and Lys–Fe–OH_2) and *c* heme proteins (His–Fe–His and His–Fe–Met ligands) (Table S4) all of which have functions associated with redox chemistry. The HPD reported values for His–Fe–NH_2 cytochromes vary considerably, from −205 mV for alkaline cytochrome *c* [64] to +350 mV for cytochrome *f* [65], a protein using the N-terminal amino group as second axial ligand. The relatively close clustering of potentials for the three THBs suggests that features beyond ligand identity play a leveling role. A relatively conserved heme environment and solvation [66] are expected to be preponderant factors in fixing the values.

The likely cognate reductase of THB1 is the diaphorase domain of NIT1. The reduction potential of the cofactors in nitrate reductase have been estimated at −280 mV for FAD, −120 to −180 mV for the *b* heme and near 0 for the Mo-pterin cofactor [67]. Given that both THB1 and THB2 are under the transcription control that regulates NIT1, nitrate transport, and assimilation, it is possible that the same diaphorase domain acts to reduce THB2 in vivo. The measured potentials place THB1 and THB2 between the potentials of the *b* heme and the Mo-pterin cofactor. Thus, Fe(III) THB1 and THB2 are a priori able to divert electrons delivered by NAD(P)H to NIT1 before they reach the active site of NIT1. At present, there is uncertainty about the expression and gene processing of THB4 so that it is unwarranted to speculate on its localization or potential physiologic reduction pathway. We do note that expression of THB4 is not linked (as with THB1 and THB2) to the expression of NIT1, and therefore it is likely that some other protein is the cognate reductase, with the abundant ferredoxin (−410 mV, [68]) as an obvious candidate.

3.6. Hemoglobin reduction under micro-oxic conditions

For comparison purposes, it is instructive to expose THB1, THB2 and THB4 to a common reduction system. We used two reductants: recombinant NIT1 flavoenzyme domain (the diaphorase domain containing no heme) [10] and NIT1 extracts from *C. reinhardtii*. Fig. 9 illustrates the time course when 50 nM flavoenzyme is used with 10 μM TrHb1. THB1 is fully reduced at a much faster rate than THB2 and THB4. Increasing the flavoenzyme concentration accelerates the rate of reduction, as expected, with THB1 reaching its reduced state faster than either THB2 or THB4 at all concentrations tested. It should be mentioned that there is no heme transfer from the TrHb1s to the apocytochrome of the diaphorase, which suggests that these proteins are not heme chaperones for nitrate reductase. When using NIT1 extracts instead of the recombinant diaphorase domain, THB1 is again reduced faster than THB2 and THB4. The ordering is THB1 > THB2 ~ THB4 (Fig. S16), although no significance can be attributed to the reversal of THB2 and THB4 in these coarse experiments.

3.7. Response of the oxygen-bound state to nitric oxide

In vitro, recombinant THB1 has the ability to perform NO dioxygenation with no damage to the heme group if catalase is included in the assay [3]. A proposed function for THB2 is also the processing of NO into nitrate, perhaps temporally separated from the same activity of THB1. The role of THB4 has not been elucidated, but a priori this protein could participate in the management of nitric oxide as well. The ability of oxy THB2 and oxy THB4 to react with NO was compared to that of oxy THB1. Fig. 10 illustrates the results of a simple assay developed for THB1. The Fe(III) protein is added to a solution containing Fd and FNR (and catalase). Upon addition of NADPH, the protein is reduced and binds oxygen. An NO donor is then added, which causes rapid oxidation of the protein, presumably as O_2 and NO combine to form nitrate. The Fe(III) protein returns to the oxy state as long as NADPH and oxygen are available and FNR is active. As can be seen in Fig. 10, all three proteins are capable of multiple NOD turnovers at neutral pH. Diminished heme absorption during the course of the NOD assay, especially apparent for THB4, is attributed to chemical damage under the conditions of the assay. Differences in the appearances of the traces are related to the different reduction rates by the ferredoxin system. The sharp loss of oxy protein upon addition of NO is similar in all three cases, within the time resolution of the experiment.

3.8. Sensitivity to hydrogen peroxide

Given the natural conditions under which THB1, THB2, and THB4 are likely to function, we inspected the response of the Fe(III) proteins to a five-fold excess of H_2O_2. Electronic absorption spectra were monitored as a function of time, with results shown in Fig. S17. In each case, a decrease of the Soret intensity is observed, but the appearance of the spectra is different. THB4 shows a slow, nearly monophasic decay, whereas THB1 and THB2 display a faster, biphasic behavior.

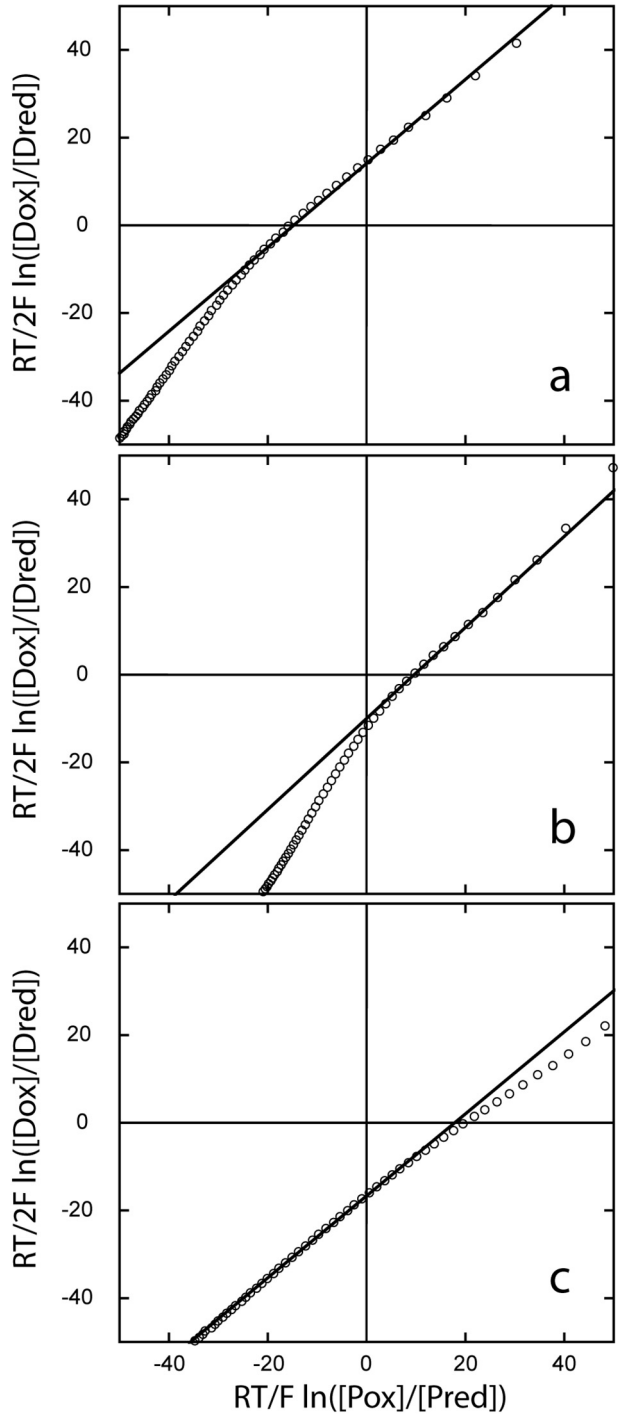

Fig. 8. Reduction potential measurements using I3S as the dye at pH 7.0 and 25 °C. (a) THB1; (b) THB2; (c) THB4. Values are obtained by adding the *y*-intercept of the linear fit to −81 mV. Inspection shows the ranking E_m(THB4) < E_m(THB2) < E_m(THB1).

Interestingly, K53A THB1 and K70A THB2 develop features characteristic of a ferryl species (Fe(IV) = O), as observed in the reaction of ferric myoglobin with H_2O_2 [69]. Even though at pH 7 the fraction of coordinated Lys E10 in THB1 and THB2 is not unity and the solvent has access to the distal site, no significant amount of ferryl species is observed in these proteins, which reflects the importance of the complexion of the distal cavity for the stabilization of the high-valent species. A detailed study is beyond the scope of this work, but it emerges that the wild-type proteins, with their compact structure and ligation scheme, can modulate reactivity toward peroxide.

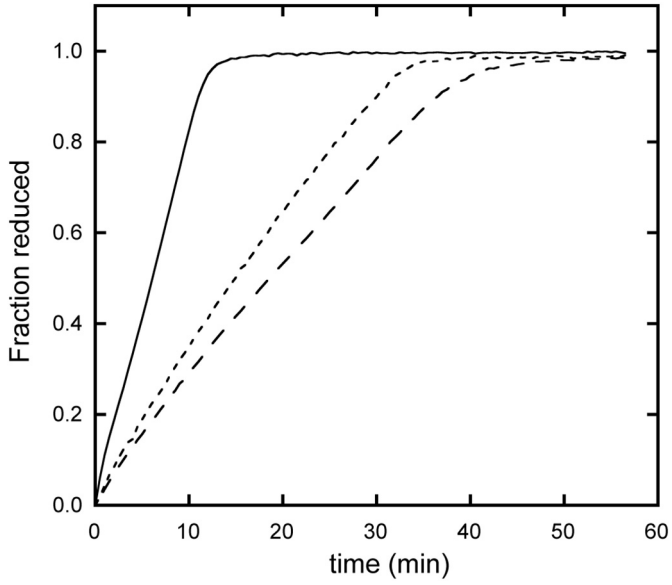

Fig. 9. Reduction of THB1 (solid line), THB2 (long dashed line) and THB4 (short dashed line) by the heme-less recombinant diaphorase domain of NIT1 (pH 7.5 and 25 °C). The fraction of reduced protein was determined by following change in absorbance value of the Soret maximum. Conditions were identical for the three proteins.

3.9. Determinants of lysine ligation

Numerous instances of Lys E10 are found in TrHb1s. So far, lysine coordination in this class of hemoglobins has been observed at neutral pH only in four *Chlamydomonas* proteins (this work and [3,5]). Identifying the determinants of endogenous distal ligation is crucial for generating functional hypotheses from globin sequences. In general, such determinants take the form of differential interactions between the ligated and unligated conformations that stabilize one form relative to the other. Electrostatic interactions between the heme propionates and basic protein residues have been proposed to serve as discriminators for ligand selection and were shown to control a competition between Lys E6 and His E10 in *Synechococcus* GlbN [44]. Protein–propionate interactions are also apparent in the His–Fe–Lys state of THB1 [5]. However, salt bridges involving the heme propionates are not observed in the structure of THB4. Unless crystal contacts are disrupting intramolecular ionic interactions, a different mechanism must be operating in this protein.

In most TrHb1s, the residue at E7 is a glutamine able to participate in a distal hydrogen bond network. In His–Fe–Lys THB4, Leu E7 contacts Phe CD1 and closes access to the distal pocket (Fig. S15) while the E helix is oriented such that Lys E10 points inside the heme cavity. *Mycobacterium tuberculosis* HbN is a relevant congener to explore the role of the residue at E7. The primary structure of HbN, like THB4, contains Lys E10, Leu E7, and Phe CD1. However, HbN has electronic absorption spectra indicative of the formation of His–Fe(III)–OH_2 and His–Fe(II) complexes in the absence of exogenous ligand [56]. Thus, the factors that control axial ligation equilibria are complex, each protein resorting to a different set of residues in the heme direct and distant periphery: THB1, THB4, and HbN illustrate the current shortcomings of homology-based predictions and reinforce the need for direct experimental verification of heme ligation states. An unexplored feature of TrHb1s is the conformational space that each protein can access under normal conditions of pH and temperature. Comparison of dynamics properties, as described for HbN [70], will contribute to clarifying the mechanism of distal ligand selection.

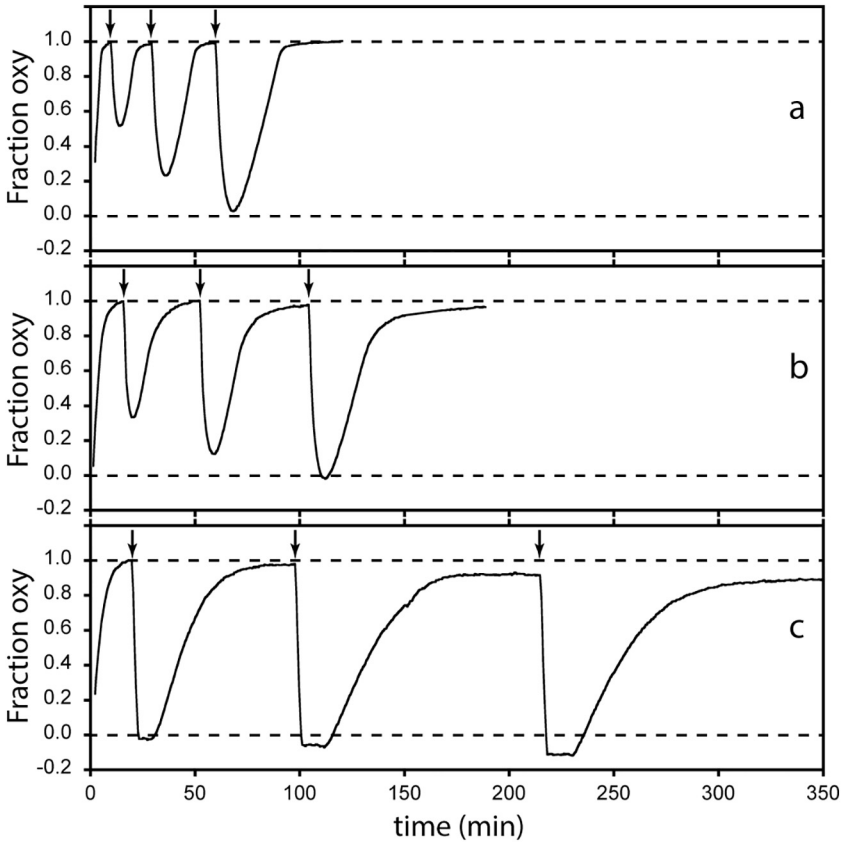

Fig. 10. Reaction of (a) THB1, (b) THB2 and (c) THB4 with NO (pH 7.5 and 25 °C). The reaction was followed by observing the absorbance of the sample at 545 nm, which reports on the proportions of Fe(II)-O_2 and Fe(III) species. In each panel, the bottom dashed line indicates the absorbance of the starting Fe(III) state; the top dashed line indicates the absorbance of the Fe(II)-O_2 state; and vertical arrows indicate NO additions.

3.10. pH response of THB1, THB2, and THB4

For proteins with ionizable axial ligands, the population of species with coordinated and decoordinated ligand depends on pH. In THB1, THB2, and THB4, the apparent pK_a of the coordinated–decoordinated equilibrium serves as a proxy for lysine affinity. Ignoring the limitations imposed by the coexistence of more than two species, it is interesting that all three proteins display a similar pH dependence of the Fe(II) state and that, at neutral pH, they show a detectable population of a deligated species capable of binding O_2, presumably rapidly [16]. Contrasting with this, the pH dependence of the Fe(III) states is variable. For example, Fe(III) THB4 has an apparent pK_a value lower than that of Fe(III) THB1 by at least 2 pH units. Whether the lower pK_a of THB4 is related to a stabilization of Lys E10 as an Fe(III) ligand or a destabilization of the alternate water-bound conformation with protonated and decoordinated Lys E10 is unclear. However, the $\Delta pK_a = pK_{a,ox} - pK_{a,red}$ (where "ox" represents the Fe(III) state of a protein and "red" the Fe(II) state of the same THB) must be related to a difference in reduction potential between the coordinated lysine THB redox pair and the decoordinated lysine THB redox pair. Conversely, the redox status of the cell is expected to modulate the proportion of ligated versus unligated lysine differently for each THB.

3.11. Biological perspective

Although lysine coordination is not commonly associated with hemoglobins, nine of the twelve TrHb1 genes in the *C. reinhardtii* genome code for lysine at E10 [71]. While most of these TrHbs have not been characterized, we have shown that at least three of these TrHbs use lysine ligation under physiological conditions. The advantages of lysine as an axial ligand in the TrHb1 scaffold include the ability to coordinate both Fe(III) and Fe(II) and setting a moderately negative reduction potential to the heme iron. A combination of these features is likely necessary for the globins to fulfill their physiologic function.

Growing interest in the NO balance within the *C. reinhardtii* cell, both in NO creation [72,73] and in its effects [74–76], has generated a consensus concerning THB1 and THB2. These proteins are thought to play a role in mitigating endogenous NO formation through dioxygenase activity sustained by nitrate reductase. Besides nitric oxide dioxygenation, many globins are capable of nitrite reduction under anaerobic conditions [77]. The reaction begins with the ferrous protein and generates NO with a concomitant loss of one electron. Not surprisingly, THB1, THB2 and THB4 are also capable of nitrite reduction [14], although a firm connection to cellular physiology is absent. Beyond the common association with nitrate reductase and NOD capability, THB1 and THB2 appear to have different physiologic expression patterns [4,78] and, as evidenced by results presented here, differing physico-chemical properties providing insight into why the cell has maintained seemingly redundant enzymes.

Temporal [79] and spatial [80] expression characteristics of other *Chlamydomonas* TrHb1s strongly suggest that nitrogen metabolism is only one of the pathways linked to these enzymes. Among other possibilities, some of these proteins may function as heme transporters. THB3 is a candidate for such activity as it exhibits weak in vitro heme association that may have benefits in vivo. Regardless, THB3 offers a first glimpse into a subclass of TrHb1s with a persistent phylogenetic presence despite lacking the key proximal histidine ligand. In addition, of two possible sequences for the N-terminal extension of THB3 (A8ISQ0 and R9S068), the second predicts mitochondrial targeting [81] and allows for new functional conjectures. Uncertainty about gene product extends to THB4, which may include a chloroplast targeting peptide [71]. Chloroplastic targeting would make THB4 a relative of LI637 (Fig. 2) [80,82], a light-induced globin of *C. eugametos* localized to the chloroplast by immunodetection. Thus, THB4 may represent a link to diurnal cycles of *C. reinhardtii* in addition to nutrient assimilation. Preliminary evidence does support diurnal cycling of THB4 [2]. Dedicated investigation into gene expression and organelle targeting will be necessary to understand fully the metabolic roles of THB3 and

THB4.

From the present study, it appears that THB1–4 have both common and distinctive physico-chemical properties. Taken together, each protein presents unique views into the structure, function and potential physiology of TrHb1s, especially in light of lysine distal ligation in THB1, THB2 and THB4. To have all four proteins exist within a single organism offers a rare chance to combine stringent in vitro characterization with in vivo exploration.

Acknowledgements

The authors thank Dagan Marx and Katelyn Jackson for protein purification and preliminary data collection, Drs. Matthew Preimesberger and Ananya Majumdar for help with NMR data collection, Dr. Katherine Tripp for assistance in the collection of circular dichroism data, Drs. Maxime Siegler and Gregory Bowman for X-ray data collection and analysis advice, and Jaime Martinez for careful reading of the manuscript. The PreScission protease was a gift of the Bowman laboratory.

Funding

This work was supported by the National Science Foundation [grant number MCB-1330488] and the National Institutes of Health [grant numbers T32 GM008403 (MMR) and GM080189 (DBN)].

Appendix A. Supplementary data

Supplementary data to this article can be found online at https://doi.org/10.1016/j.bbagen.2018.08.009.

References

[1] A. Hemschemeier, D. Casero, B. Liu, C. Benning, M. Pellegrini, T. Happe, S.S. Merchant, Copper response regulator1-dependent and -independent responses of the *Chlamydomonas reinhardtii* transcriptome to dark anoxia, Plant Cell 25 (2013) 3186–3211, https://doi.org/10.1105/tpc.113.115741.

[2] J.M. Zones, I.K. Blaby, S.S. Merchant, J.G. Umen, High-resolution profiling of a synchronized diurnal transcriptome from *Chlamydomonas reinhardtii* reveals continuous cell and metabolic differentiation, Plant Cell 27 (2015) 2743–2769, https://doi.org/10.1105/tpc.15.00498.

[3] E.A. Johnson, S.L. Rice, M.R. Preimesberger, D.B. Nye, L. Gilevicius, B.B. Wenke, J.M. Brown, G.B. Witman, J.T.J. Lecomte, Characterization of THB1, a *Chlamydomonas reinhardtii* truncated hemoglobin: linkage to nitrogen metabolism and identification of lysine as the distal heme ligand, Biochemistry 53 (2014) 4573–4589, https://doi.org/10.1021/bi5005206.

[4] E. Sanz-Luque, F. Ocaña-Calahorro, A. de Montaigu, A. Chamizo-Ampudia, A. Llamas, A. Galvan, E. Fernández, THB1, a truncated hemoglobin, modulates nitric oxide levels and nitrate reductase activity, Plant J. 81 (2015) 467–479, https://doi.org/10.1111/tpj.12744.

[5] S.L. Rice, L.E. Boucher, J.L. Schlessman, M.R. Preimesberger, J. Bosch, J.T.J. Lecomte, Structure of *Chlamydomonas reinhardtii* THB1, a group 1 truncated hemoglobin with a rare histidine-lysine heme ligation, Acta Crystallogr. F Struct. Biol. Commun. 71 (2015) 718–725, https://doi.org/10.1107/S2053230X15006949.

[6] M.R. Preimesberger, A. Majumdar, J.T.J. Lecomte, Dynamics of lysine as a heme axial ligand: NMR analysis of the *Chlamydomonas reinhardtii* hemoglobin THB1, Biochemistry 56 (2017) 551–569, https://doi.org/10.1021/acs.biochem.6b00926.

[7] K. Tsukahara, Kinetics and mechanisms of reduction of metmyoglobins - Importance of the geometry change at the heme iron site upon reduction, J. Am. Chem. Soc. 111 (1989) 2040–2044, https://doi.org/10.1021/ja00188a014.

[8] A. Pesce, M. Couture, S. Dewilde, M. Guertin, K. Yamauchi, P. Ascenzi, L. Moens, M. Bolognesi, A novel two-over-two α-helical sandwich fold is characteristic of the truncated hemoglobin family, EMBO J. 19 (2000) 2424–2434, https://doi.org/10.1093/emboj/19.11.2424.

[9] H. Ouellet, Y. Ouellet, C. Richard, M. Labarre, B. Wittenberg, J. Wittenberg, M. Guertin, Truncated hemoglobin HbN protects *Mycobacterium bovis* from nitric oxide, Proc. Natl. Acad. Sci. U. S. A. 99 (2002) 5902–5907, https://doi.org/10.1073/pnas.092017799.

[10] M.R. Preimesberger, E.A. Johnson, D.B. Nye, J.T.J. Lecomte, Covalent attachment of the heme to *Synechococcus* hemoglobin alters its reactivity toward nitric oxide, J. Inorg. Biochem. 177 (2017) 171–182, https://doi.org/10.1016/j.jinorgbio.2017.09.018.

[11] D. Giordano, A. Pesce, L. Boechi, J.P. Bustamante, E. Caldelli, B.D. Howes, A. Riccio, G. di Prisco, M. Nardini, D. Estrin, G. Smulevich, M. Bolognesi, C. Verde, Structural flexibility of the heme cavity in the cold-adapted truncated hemoglobin from the Antarctic marine bacterium *Pseudoalteromonas haloplanktis* TAC125, FEBS J. 282 (2015) 2948–2965, https://doi.org/10.1111/febs.13335.

[12] S. Saroussi, E. Sanz-Luque, R.G. Kim, A.R. Grossman, Nutrient scavenging and energy management: acclimation responses in nitrogen and sulfur deprived *Chlamydomonas*, Curr. Op. Plant Biol. 39 (2017) 114–122, https://doi.org/10.1016/j.pbi.2017.06.002.

[13] S.N. Vinogradov, M. Tinajero-Trejo, R.K. Poole, D. Hoogewijs, Bacterial and archaeal globins — A revised perspective, Biochim. Biophys. Acta 1834 (2013) 1789–1800, https://doi.org/10.1016/j.bbapap.2013.03.021.

[14] C. Ciaccio, F. Ocaña-Calahorro, E. Droghetti, G.R. Tundo, E. Sanz-Luque, F. Polticelli, P. Visca, G. Smulevich, P. Ascenzi, M. Coletta, Functional and spectroscopic characterization of *Chlamydomonas reinhardtii* truncated hemoglobins, PLoS One 10 (2015) e0125005, , https://doi.org/10.1371/journal.pone.0125005.

[15] M. Johnson, I. Zaretskaya, Y. Raytselis, Y. Merezhuk, S. McGinnis, T.L. Madden, NCBI BLAST: a better web interface, Nucleic Acids Res. 36 (2008) W5–W9, https://doi.org/10.1093/nar/gkn201.

[16] B.J. Smagghe, P. Halder, M.S. Hargrove, Measurement of distal histidine coordination equilibrium and kinetics in hexacoordinate hemoglobins, Methods Enzymol. 436 (2008) 359–378, https://doi.org/10.1016/S0076-6879(08)36020-0.

[17] Q. Xiao, F. Zhang, B.A. Nacev, J.O. Liu, D. Pei, Protein N-terminal processing: Substrate specificity of *Escherichia coli* and human methionine aminopeptidases, Biochemistry 49 (2010) 5588–5599, https://doi.org/10.1021/bi1005464.

[18] E.A. Johnson, J.T.J. Lecomte, Characterization of the truncated hemoglobin THB1 from protein extracts of *Chlamydomonas reinhardtii*, F1000Research 3 (2014) 294, https://doi.org/10.12688/f1000research.5873.1.

[19] K. Fiege, C.J. Querebillo, P. Hildebrandt, N. Frankenberg-Dinkel, Improved method for the incorporation of heme-cofactors into recombinant proteins using *Escherichia coli* Nissle 1917, Biochemistry (2018), https://doi.org/10.1021/acs.biochem.8b00242 in press.

[20] B.J. Reeder, D.A. Svistunenko, M.T. Wilson, Lipid binding to cytoglobin leads to a change in haem co-ordination: a role for cytoglobin in lipid signalling of oxidative stress, Biochem. J. 434 (2011) 483–492, https://doi.org/10.1042/bj20101136.

[21] K.G. Paul, H. Theorell, A. Akeson, The molar light absorption of pyridine ferroprotoporphyrin (pyridine haemochromogen), Acta Chem. Scan. 7 (1953) 1284–1287.

[22] A.R. Franco, J. Cardenas, E. Fernández, Heteromultimeric structure of the nitrate reductase complex of *Chlamydomonas reinhardii*, EMBO J. 3 (1984) 1403–1407.

[23] P. Griess, Bemerkungen zu der Abhandlung der HH Weselsky und Benedikt "Über einige Azoverbindungen", Chem. Ber. 12 (1879) 426–428.

[24] M. Couture, T.K. Das, H.C. Lee, J. Peisach, D.L. Rousseau, B.A. Wittenberg, J.B. Wittenberg, M. Guertin, *Chlamydomonas* chloroplast ferrous hemoglobin. Heme pocket structure and reactions with ligands, J. Biol. Chem. 274 (1999) 6898–6910, https://doi.org/10.1074/jbc.274.11.6898.

[25] V. Massey, A simple method for the determination of redox potentials, in: B. Curti, S. Ronchi, G. Zanetti (Eds.), Flavins and Flavoproteins 1990, Walter de Gruyter & Co., Berlin, New York, 1991, pp. 59–66.

[26] I. Efimov, G. Parkin, E.S. Millett, J. Glenday, C.K. Chan, H. Weedon, H. Randhawa, J. Basran, E.L. Raven, A simple method for the determination of reduction potentials in heme proteins, FEBS Lett. 588 (2014) 701–704, https://doi.org/10.1016/j.febslet.2013.12.030.

[27] R. Wurmser, Oxidation-reduction potentials, Comp. Biochem. 12 (1964) 62–88.

[28] A. Hayashi, T. Suzuki, M. Shin, An enzymic reduction system for metmyoglobin and methemoglobin, and its application to functional studies of oxygen carriers, Biochim. Biophys. Acta 310 (1973) 309–316, https://doi.org/10.1016/0005-2795(73)90110-4.

[29] D.P. Nelson, L.A. Kiesow, Enthalpy of decomposition of hydrogen peroxide by catalase at 25 degrees C (with molar extinction coefficients of H_2O_2 solutions in the UV), Anal. Biochem. 49 (1972) 474–478, https://doi.org/10.1016/0003-2697(72)90451-4.

[30] E.E. Di Iorio, Preparation of derivatives of ferrous and ferric hemoglobin, Methods Enzymol. 76 (1981) 57–72, https://doi.org/10.1016/0076-6879(81)76114-7.

[31] D.S. Wishart, C.G. Bigam, J. Yao, F. Abildgaard, H.J. Dyson, E. Oldfield, J.L. Markley, B.D. Sykes, ^{1}H, ^{13}C and ^{15}N chemical shift referencing in biomolecular NMR, J. Biomol. NMR 6 (1995) 135–140, https://doi.org/10.1007/BF00211777.

[32] F. Delaglio, S. Grzesiek, G.W. Vuister, G. Zhu, J. Pfeifer, A. Bax, NMRPipe: a multidimensional spectral processing system based on UNIX pipes, J. Biomol. NMR 6 (1995) 277–293, https://doi.org/10.1007/BF00197809.

[33] T.D. Goddard, D.G. Kneller, SPARKY 3, University of California, San Francisco, 2006.

[34] D. Lee, C. Hilty, G. Wider, K. Wüthrich, Effective rotational correlation times of proteins from NMR relaxation interference, J. Magn. Reson. 178 (2006) 72–76, https://doi.org/10.1016/j.jmr.2005.08.014.

[35] M.P. Pond, A. Majumdar, J.T.J. Lecomte, Influence of heme post-translational modification and distal ligation on the backbone dynamics of a monomeric hemoglobin, Biochemistry 51 (2012) 5733–5747, https://doi.org/10.1021/bi300624a.

[36] P.D. Adams, P.V. Afonine, G. Bunkoczi, V.B. Chen, I.W. Davis, N. Echols, J.J. Headd, L.W. Hung, G.J. Kapral, R.W. Grosse-Kunstleve, A.J. McCoy, N.W. Moriarty, R. Oeffner, R.J. Read, D.C. Richardson, J.S. Richardson, T.C. Terwilliger, P.H. Zwart, PHENIX: a comprehensive Python-based system for macromolecular structure solution, Acta Crystallogr. D Biol. Crystallogr. 66 (2010) 213–221, https://doi.org/10.1107/S0907444909052925.

[37] P. Emsley, B. Lohkamp, W.G. Scott, K. Cowtan, Features and development of Coot, Acta Crystallogr. D Biol. Crystallogr. 66 (2010) 486–501, https://doi.org/10.1107/S0907444910007493.

[38] E. Krissinel, K. Henrick, Inference of macromolecular assemblies from crystalline state, J. Mol. Biol. 372 (2007) 774–797, https://doi.org/10.1016/j.jmb.2007.05.022.

[39] K. Berka, O. Hanák, D. Sehnal, P. Banáš, V. Navrátilová, D. Jaiswal, C. Ionescu, R. Svobodová Vařeková, J. Koča, M. Otyepka, MOLEonline 2.0: interactive web-based analysis of biomacromolecular channels, Nucleic Acids Res. 40 (2012) W222–W227, https://doi.org/10.1093/nar/gks363.

[40] A. Bonamore, A. Ilari, L. Giangiacomo, A. Bellelli, V. Morea, A. Boffi, A novel thermostable hemoglobin from the actinobacterium *Thermobifida fusca*, FEBS J. 272 (2005) 4189–4201, https://doi.org/10.1111/j.1742-4658.2005.04831.x.

[41] A. Ilari, P. Kjelgaard, C. von Wachenfeldt, B. Catacchio, E. Chiancone, A. Boffi, Crystal structure and ligand binding properties of the truncated hemoglobin from *Geobacillus stearothermophilus*, Arch. Biochem. Biophys. 457 (2007) 85–94, https://doi.org/10.1016/j.abb.2006.09.033.

[42] E. Antonini, M. Brunori, Hemoglobin, Annu. Rev. Biochem. 39 (1970) 977–1042.

[43] M. Ubbink, A.P. Campos, M. Teixeira, N.I. Hunt, H.A. Hill, G.W. Canters, Characterization of mutant Met100Lys of cytochrome *c*-550 from *Thiobacillus versutus* with lysine-histidine heme ligation, Biochemistry 33 (1994) 10051–10059, https://doi.org/10.1021/bi00199a032.

[44] D.B. Nye, M.R. Preimesberger, A. Majumdar, J.T.J. Lecomte, Histidine–lysine axial ligand switching in a hemoglobin: A role for heme propionates, Biochemistry 57 (2018) 631–644, https://doi.org/10.1021/acs.biochem.7b01155.

[45] H.M. Girvan, H.S. Toogood, R.E. Littleford, H.E. Seward, W.E. Smith, I.S. Ekanem, D. Leys, M.R. Cheesman, A.W. Munro, Novel haem co-ordination variants of flavocytochrome P450 BM3, Biochem. J. 417 (2009) 65–80, https://doi.org/10.1042/bj20081133.

[46] L. Milazzo, S. Hofbauer, B.D. Howes, T. Gabler, P.G. Furtmuller, C. Obinger, G. Smulevich, Insights into the active site of coproheme decarboxylase from *Listeria monocytogenes*, Biochemistry (2018), https://doi.org/10.1021/acs.biochem.8b00186.

[47] H.H. Brewitz, G. Hagelueken, D. Imhof, Structural and functional diversity of transient heme binding to bacterial proteins, Biochim. Biophys. Acta 1861 (2017) 683–697, https://doi.org/10.1016/j.bbagen.2016.12.021.

[48] H.J. Nothnagel, B.Y. Winer, D.A. Vuletich, M.P. Pond, J.T.J. Lecomte, Structural properties of 2/2 hemoglobins: The group III protein from *Helicobacter hepaticus*, IUBMB Life 63 (2011) 197–205, https://doi.org/10.1002/iub.430.

[49] W.L. Delano, The PyMOL Molecular Graphics System, in, DeLano Scientific, San Carlos, CA, USA, 2002.

[50] B.B. Wenke, J.T.J. Lecomte, A. Héroux, J.L. Schlessman, The 2/2 hemoglobin from the cyanobacterium *Synechococcus* sp. PCC 7002 with covalently attached heme: comparison of X-ray and NMR structures, Proteins 82 (2014) 528–534, https://doi.org/10.1002/prot.24409.

[51] W. Jentzen, J.G. Ma, J.A. Shelnutt, Conservation of the conformation of the porphyrin macrocycle in hemoproteins, Biophys. J. 74 (1998) 753–763, https://doi.org/10.1016/S0006-3495(98)74000-7.

[52] U. Samuni, Y. Ouellet, M. Guertin, J.M. Friedman, S.R. Yeh, The absence of proximal strain in the truncated hemoglobins from *Mycobacterium tuberculosis*, J. Am. Chem. Soc. 126 (2004) 2682–2683, https://doi.org/10.1021/ja038093i.

[53] D.A. Vuletich, J.T.J. Lecomte, A phylogenetic and structural analysis of truncated hemoglobins, J. Mol. Evol. 62 (2006) 196–210, https://doi.org/10.1007/s00239-005-0077-4.

[54] M.R. Preimesberger, A. Majumdar, S.L. Rice, L. Que, J.T.J. Lecomte, Helix-capping histidines: Diversity of N-H...N hydrogen bond strength revealed by $^{2h}J_{NN}$ scalar couplings, Biochemistry 54 (2015) 6896–6908, https://doi.org/10.1021/acs.biochem.5b01002.

[55] N.L. Scott, C.J. Falzone, D.A. Vuletich, J. Zhao, D.A. Bryant, J.T.J. Lecomte, The hemoglobin of the cyanobacterium *Synechococcus* sp. PCC 7002: Evidence for hexacoordination and covalent adduct formation in the ferric recombinant protein, Biochemistry 41 (2002) 6902–6910, https://doi.org/10.1021/bi025609m.

[56] M. Couture, S.R. Yeh, B.A. Wittenberg, J.B. Wittenberg, Y. Ouellet, D.L. Rousseau, M. Guertin, A cooperative oxygen-binding hemoglobin from *Mycobacterium tuberculosis*, Proc. Natl. Acad. Sci. U. S. A. 96 (1999) 11223–11228, https://doi.org/10.1073/pnas.96.20.11223.

[57] J. Igarashi, K. Kobayashi, A. Matsuoka, A hydrogen-bonding network formed by the B10-E7-E11 residues of a truncated hemoglobin from *Tetrahymena pyriformis* is critical for stability of bound oxygen and nitric oxide detoxification, J. Biol. Inorg. Chem. 16 (2011) 599–609, https://doi.org/10.1007/s00775-011-0761-3.

[58] M. Milani, A. Pesce, Y. Ouellet, S. Dewilde, J. Friedman, P. Ascenzi, M. Guertin, M. Bolognesi, Heme-ligand tunneling in group I truncated hemoglobins, J. Biol. Chem. 279 (2004) 21520–21525, https://doi.org/10.1074/jbc.M401320200.

[59] J.T. Trent 3rd, S. Kundu, J.A. Hoy, M.S. Hargrove, Crystallographic analysis of *Synechocystis* cyanoglobin reveals the structural changes accompanying ligand binding in a hexacoordinate hemoglobin, J. Mol. Biol. 341 (2004) 1097–1108, https://doi.org/10.1016/j.jmb.2004.05.070.

[60] A. Crespo, M.A. Marti, S.G. Kalko, A. Morreale, M. Orozco, J.L. Gelpi, F.J. Luque, D.A. Estrin, Theoretical study of the truncated hemoglobin HbN: exploring the molecular basis of the NO detoxification mechanism, J. Am. Chem. Soc. 127 (2005) 4433–4444, https://doi.org/10.1021/ja0450004.

[61] R. Daigle, M. Guertin, P. Lagüe, Structural characterization of the tunnels of *Mycobacterium tuberculosis* truncated hemoglobin N from molecular dynamics simulations, Proteins 75 (2009) 735–747, https://doi.org/10.1002/prot.22283.

[62] S.W. Englander, D.B. Calhoun, J.J. Englander, Biochemistry without oxygen, Anal. Biochem. 161 (1987) 300–306, https://doi.org/10.1016/0003-2697(87)90454-4.

[63] C.J. Reedy, M.M. Elvekrog, B.R. Gibney, Development of a heme protein structure-electrochemical function database, Nucleic Acids Res. 36 (2008) D307–D313, https://doi.org/10.1093/nar/gkm814.

[64] P.D. Barker, A.G. Mauk, pH-Linked conformational regulation of a metalloprotein oxidation-reduction equilibrium: electrochemical analysis of the alkaline form of cytochrome *c*, J. Am. Chem. Soc. 114 (1992) 3619–3624, https://doi.org/10.1021/ja00036a006.

[65] S.E. Martinez, D. Huang, M. Ponomarev, W.A. Cramer, J.L. Smith, The heme redox center of chloroplast cytochrome *f* is linked to a buried five-water chain, Protein Sci. 5 (1996) 1081–1092, https://doi.org/10.1002/pro.5560050610.

[66] Z. Zheng, M.R. Gunner, Analysis of the electrochemistry of hemes with E_ms spanning 800 mV, Proteins 75 (2009) 719–734, https://doi.org/10.1002/prot.22282.

[67] W.H. Campbell, Nitrate reductase structure, function and regulation: Bridging the Gap between Biochemistry and Physiology, Annu. Rev. Plant Physiol. Plant Mol. Biol. 50 (1999) 277–303, https://doi.org/10.1146/annurev.arplant.50.1.277.

[68] F. Galván, J. Márquez Antonio, E. Fernández, Physicochemical properties of ferredoxin from *Chlamydomonas reinhardii*, Z. Naturforsch. C Bio. Sci. 40 (1985) 373, https://doi.org/10.1515/znc-1985-5-615.

[69] C. Giulivi, E. Cadenas, Ferrylmyoglobin: Formation and chemical reactivity toward electron-donating compounds, Methods Enzymol. 233 (1994) 189–202, https://doi.org/10.1016/S0076-6879(94)33022-0.

[70] P.Y. Savard, R. Daigle, S. Morin, A. Sebilo, F. Meindre, P. Lagüe, M. Guertin, S.M. Gagné, Structure and dynamics of *Mycobacterium tuberculosis* truncated hemoglobin N: insights from NMR spectroscopy and molecular dynamics simulations, Biochemistry 50 (2011) 11121–11130, https://doi.org/10.1021/bi201059a.

[71] E.A. Johnson, J.T.J. Lecomte, The haemoglobins of algae, Adv. Microb. Physiol. 67 (2015) 177–234, https://doi.org/10.1016/bs.ampbs.2015.08.003.

[72] A. Chamizo-Ampudia, E. Sanz-Luque, A. Llamas, F. Ocaña-Calahorro, V. Mariscal, A. Carreras, J.B. Barroso, A. Galván, E. Fernández, A dual system formed by the ARC and NR molybdoenzymes mediates nitrite-dependent NO production in *Chlamydomonas*, Plant Cell Environ. 39 (2016) 2097–2107, https://doi.org/10.1111/pce.12739.

[73] J. Astier, I. Gross, J. Durner, Nitric oxide production in plants: an update, J. Exp. Bot. 69 (2018) 3401–3411, https://doi.org/10.1093/jxb/erx420.

[74] Z. Zalutskaya, M. Ostroukhova, V. Filina, E. Ermilova, Nitric oxide upregulates expression of alternative oxidase 1 in *Chlamydomonas reinhardtii*, J. Plant Physiol. 219 (2017) 123–127, https://doi.org/10.1016/j.jplph.2017.10.004.

[75] W. Pokora, A. Aksmann, A. Bascik-Remisiewicz, A. Dettlaff-Pokora, M. Rykaczewski, M. Gappa, Z. Tukaj, Changes in nitric oxide/hydrogen peroxide content and cell cycle progression: Study with synchronized cultures of green alga *Chlamydomonas reinhardtii*, J. Plant Physiol. 208 (2017) 84–93, https://doi.org/10.1016/j.jplph.2016.10.008.

[76] M. Plouviez, D. Wheeler, A. Shilton, M.A. Packer, P.A. McLenachan, E. Sanz-Luque, F. Ocaña-Calahorro, E. Fernández, B. Guieysse, The biosynthesis of nitrous oxide in the green alga *Chlamydomonas reinhardtii*, Plant J. 91 (2017) 45–56, https://doi.org/10.1111/tpj.13544.

[77] R. Sturms, A.A. Dispirito, M.S. Hargrove, Plant and cyanobacterial hemoglobins reduce nitrite to nitric oxide under anoxic conditions, Biochemistry 50 (2011) 3873–3878, https://doi.org/10.1021/bi2004312.

[78] E. Minaeva, Z. Zalutskaya, V. Filina, E. Ermilova, Truncated hemoglobin 1 is a new player in *Chlamydomonas reinhardtii* acclimation to sulfur deprivation, PLoS One 12 (2017) e0186851, , https://doi.org/10.1371/journal.pone.0186851.

[79] A. Hemschemeier, M. Duner, D. Casero, S.S. Merchant, M. Winkler, T. Happe, Hypoxic survival requires a 2-on-2 hemoglobin in a process involving nitric oxide, Proc. Natl. Acad. Sci. U. S. A. 110 (2013) 10854–10859, https://doi.org/10.1073/pnas.1302592110.

[80] G. Gagné, M. Guertin, The early genetic response to light in the green unicellular alga *Chlamydomonas eugametos* grown under light dark cycles involves genes that represent direct responses to light and photosynthesis, Plant Mol. Biol. 18 (1992) 429–445, https://doi.org/10.1007/Bf00040659.

[81] M. Tardif, A. Atteia, M. Specht, G. Cogne, N. Rolland, S. Brugière, M. Hippler, M. Ferro, C. Bruley, G. Peltier, O. Vallon, L. Cournac, PredAlgo: A new subcellular localization prediction tool dedicated to green algae, Mol. Biol. Evol. 29 (2012) 3625–3639, https://doi.org/10.1093/molbev/mss178.

[82] M. Couture, H. Chamberland, B. St-Pierre, J. Lafontaine, M. Guertin, Nuclear genes encoding chloroplast hemoglobins in the unicellular green alga *Chlamydomonas eugametos*, Mol. Gen. Genet. 243 (1994) 185–197, https://doi.org/10.1007/BF00280316.